SIAM J. APPL. MATH.
Vol. 85, No. 3, pp. 1287–1313




# RANDOM WALKS OF SWARMING ON MONOTONIC RESOURCE DISTRIBUTION IN A LANDSCAPE*

ZHENFENG SHI†, DAQING JIANG‡, AND HAO WANG§

**Abstract.** This study introduces a novel resource-consumer model that uniquely integrates stochastic consumer movement with spatially monotonic resource distributions, advancing our understanding of consumer dynamics in heterogeneous environments. In this framework, swarming consumer movement within a home range is modeled using the Ornstein–Uhlenbeck process, realistically capturing random walks within home range. By accounting for resource heterogeneity, the model enables consumers to access variable resource levels based on location, offering a fresh approach to simulating consumer-resource interactions in spatially structured landscapes. Key contributions include the derivation of the consumption threshold that determines the asymptotic behavior of the consumer population, distinguishing scenarios of persistence, and extinction. In addition, a novel control function is constructed to rigorously establish the existence and uniqueness of the invariant density.

**Key words.** random walk, home range, resource-consumer dynamics, swarming, heterogeneity

**MSC codes.** 34F05, 60H10, 92B05, 92D25

**DOI.** 10.1137/24M1708826

## 1. Introduction.

The dynamics between resources and consumers are a fundamental aspect of ecological systems, involving interactions between organisms that consume resources and the spatial and temporal availability of those resources within their environment [9]. In natural ecosystems, resources like food and water are rarely uniformly distributed; instead, they often exhibit monotonic heterogeneity, where availability gradually changes across the landscape [32]. This spatial variation compels consumers to engage in collective movement behaviors, such as flocking, herding, or schooling, to more effectively locate, access, and utilize these unevenly distributed resources [16]. Such collective movements not only improve the ability of consumers to exploit resource patches but also provide adaptive advantages in facing predation risks and environmental changes [53]. Therefore, understanding the complex interplay between resource distribution and consumer movement is crucial for predicting population dynamics, maintaining ecosystem stability, and developing effective ecological management strategies.

*Received by the editors November 8, 2024; accepted for publication (in revised form) March 3, 2025; published electronically June 23, 2025.
https://doi.org/10.1137/24M1708826
**Funding:** The work of the first author was partially supported by Program of China Scholarship Council grant 202306620088. The work of the second author was partially supported by National Natural Science Foundation of China grant 11871473 and by Fundamental Research Funds for the Central Universities grant 22CX03030A. The work of the third author was partially supported by Natural Sciences and Engineering Research Council of Canada Individual Discovery grant RGPIN-2020-03911 and Discovery Accelerator Supplement award RGPAS-2020-00090, and by a Canada Research Chair.

†Department of Biostatistics, School of Public Health, Southern Medical University, Guangzhou, Guangdong, 510515 China (shizhenfeng95@163.com).
‡College of Science, China University of Petroleum, Qingdao, Shandong, 266580 China (daqingjiang2010@hotmail.com).
§Corresponding author: Department of Mathematical and Statistical Sciences & Interdisciplinary Lab for Mathematical Ecology and Epidemiology, University of Alberta, Edmonton, Alberta T6G 2G1, Canada (hao8@ualberta.ca).

Consumer groups often have a defined home location, with most of their movements restricted to a specific home range—a behavior observed across many animal species [39]. The home range is an area where individuals or groups conduct regular activities, such as foraging, mating, and sheltering, typically centered around a home location [47]. This spatial constraint results from a mix of ecological and behavioral factors. For instance, species like mammals [34, 44], birds [6, 35], fish [23], and insects [56, 3] show site fidelity, consistently returning to familiar areas that provide reliable resources or protection from predators. This behavior enhances resource use efficiency, reduces risks in unfamiliar environments, and improves survival by minimizing exposure to threats. Additionally, staying within a home range helps establish and maintain social structures, territories, and mating systems, which are crucial for species fitness and reproduction. Understanding these movement patterns is vital for modeling the spatial dynamics of consumer-resource interactions in ecological research.

Swarming is a type of collective movement observed in many consumer species, where group members coordinate their movements to achieve common goals, such as locating food, avoiding predators, or migrating [13, 40]. This behavior is particularly common in species that face spatially heterogeneous resources, as swarming enables efficient searching and exploitation of unevenly distributed resource patches [34]. However, decision making within swarming groups often involves randomness due to several factors: environmental unpredictability (such as fluctuating weather or the presence of predators), divergence in movement preferences among group members, inherent behavioral diversity, and the quality of communication [37]. Together, these factors create a dynamic and adaptive system in which group movement remains both coordinated and flexible, enhancing the ability of the group to respond to complex and changing environments.

The random walk of consumer groups within a home range can be effectively modeled using stochastic differential equations (SDEs), which capture inherent randomness in movement patterns beyond the scope of ordinary or partial differential equations [5, 7, 50, 52]. The Ornstein–Uhlenbeck (OU) process is a widely used SDE for modeling such movements, providing a framework to describe consumer dynamics [14]. In this process, the mean term represents the home location, acting as an attractor, while the mean reversion rate reflects the strength of this attraction [8]. The noise term captures stochastic fluctuations, accounting for the inherent randomness in consumer movements.

This mathematical approach models both the tendency of consumers to stay near their home location and the randomness in their movements due to environmental variability or individual choices. By balancing attraction to a central location with random exploration, the OU process effectively represents realistic animal movements observed in nature [12]. Furthermore, adjusting parameters like the mean reversion rate and noise intensity allows the model to accommodate various ecological scenarios, from stable home ranges with minimal deviations to dynamic environments with unpredictable movements. This flexibility makes the OU-based SDE approach a valuable tool for understanding and predicting consumer-resource interactions in heterogeneous landscapes [20].

Despite advances in ecological modeling, many existing resource-consumer models struggle to capture the intrinsic randomness of consumer movements and the complex spatial heterogeneity of resource landscapes. Traditional models often assume uniformly random or predetermined movement paths, failing to reflect the adaptive nature of real-world behaviors [10]. These simplifications create gaps in understanding

how consumers interact with spatially and temporally varying resources, particularly in heterogeneous environments where resources are unevenly distributed and constantly changing [43, 11]. Additionally, environmental fluctuations and behavioral diversity, which are crucial for population dynamics and resource stability, are often overlooked.

Integrating stochastic random walks into resource-consumer models is essential for capturing the complex dynamics of ecosystems, where consumers move between varying resource locations [31]. Resource availability fluctuates significantly based on the specific locations visited by consumer groups. By incorporating random walk behavior, modeled using the OU process, with classical resource-consumer frameworks, we can more accurately represent the spatial and temporal heterogeneity of resources and its impact on consumer populations. This integrated approach offers a more realistic simulation of how consumer movements influence resource consumption, population stability, and overall ecosystem dynamics [15].

This study addresses these limitations by incorporating stochastic movement patterns and spatially explicit resource distributions into resource-consumer models. Using random walks defined by SDEs provides a more realistic framework to represent how consumer groups respond to diverse environmental conditions and fluctuating resource availability. This approach improves the predictive capacity of ecological models and facilitates deeper exploration of the conditions under which consumer populations persist, compete, or coexist. Ultimately, this research bridges the gap between theoretical models and observed ecological phenomena, enabling more accurate predictions and better management of natural resources.

The rest of this paper is organized as follows: Section 2 defines the stochastic random walk using the OU process and introduces the associated resource-consumer model. Section 3 explores the long-term dynamics of the stochastic model, including the existence and uniqueness of the global solution, stochastic consumption threshold dynamics, and the local probability density function. Section 4 presents numerical simulations that validate the analysis and highlight interesting findings. Finally, section 5 summarizes the main results of the study.

## 2. Model formulation.

**2.1. Random walk within home range.** In this paper, we generalize the classical OU process to three-dimensional space, providing a framework for modeling stochastic dynamics along three independent spatial axes. The SDE describing the three-dimensional OU process is given by

$$\mathrm{d}\mathbf{X}_t = \boldsymbol{\theta}(\boldsymbol{\mu} - \mathbf{X}_t)\mathrm{d}t + \boldsymbol{\sigma}\mathrm{d}\mathbf{B}_t,$$

where the following hold:

- $\mathbf{X}_t = \begin{pmatrix} X_t^x \\ X_t^y \\ X_t^z \end{pmatrix}$ is the three-dimensional state vector, representing the real-time location of a consumer group (considered as a point relative to their movement scale) along each axis at time $t$.
- $\boldsymbol{\mu} = \begin{pmatrix} \mu_x \\ \mu_y \\ \mu_z \end{pmatrix}$ is the home location of consumers.
- $\mathbf{B}_t = \begin{pmatrix} B_t^x \\ B_t^y \\ B_t^z \end{pmatrix}$ represents the vector of independent Brownian motions.
- $\boldsymbol{\theta} = \mathrm{diag}(\theta_x, \theta_y, \theta_z)$ denotes the attractiveness of the home location.
- $\boldsymbol{\sigma} = \mathrm{diag}(\sigma_x, \sigma_y, \sigma_z)$ represents the intensity of the random walk.

The steady-state distribution of the location vector follows a multivariate normal distribution:

$$(X^x, X^y, X^z) \sim \mathbb{N}\left((\bar{x}, \bar{y}, \bar{z}), \operatorname{diag}\left(\frac{\sigma_x^2}{2\theta_x}, \frac{\sigma_y^2}{2\theta_y}, \frac{\sigma_z^2}{2\theta_z}\right)\right).$$

The confidence level can be used to define the home range of consumers, encompassing the majority of their random movements within a spatial region. Specifically, for a given confidence level $1-\alpha$, the home range is the region where the consumers are expected to remain most of the time:

$$\left(\frac{2\theta_x(X^x-\mu_x)}{\sigma_x^2} + \frac{2\theta_y(X^y-\mu_y)}{\sigma_y^2} + \frac{2\theta_z(X^z-\mu_z)}{\sigma_z^2}\right) \le \chi^2_{3,1-\alpha},$$

which reflects the bounds within which their random walks are predominantly confined. The three-dimensional OU process effectively models the random movement of aquatic organisms like plankton, which swarm within a three-dimensional environment. Conversely, the two-dimensional OU process is suited for terrestrial or surface-dwelling organisms, such as land animals or organisms on the water surface.

**2.2. Stochastic resource-consumer model.** Consider a scenario in which resource availability is influenced by a one-dimensional spatial factor, such as the gradual change in resource distribution along varying latitudes. In this setting, resources are distributed nonuniformly, exhibiting a monotonic variation across a single spatial dimension. This spatial heterogeneity causes differences in resource accessibility for consumers moving stochastically along the gradient. Modeling consumer movement as a stochastic process on this spatial axis allows us to explore how environmental factors, such as latitude, influence resource availability and, in turn, impact consumer behavior and population dynamics. Denote

$$\mathrm{d}x(t) = \theta(\bar{x} - x(t))\mathrm{d}t + \sigma \mathrm{d}B(t),$$

where $x(t)$ represents the location of the consumer population at time $t$, $\bar{x}$ is the home location of the consumer population, $\theta$ denotes the home attractiveness, $\sigma$ represents the intensity of random walk, and $B(t)$ denotes one-dimensional standard Brownian motion. Given that $x \sim \mathbb{N}(\bar{x}, \frac{\sigma^2}{2\theta})$ [1], the 95% confidence interval is

$$\left[\bar{x} - 1.96\sqrt{\frac{\sigma^2}{2\theta}}, \bar{x} + 1.96\sqrt{\frac{\sigma^2}{2\theta}}\right].$$

Figure 1 illustrates the range of consumer movement under different parameter values, where higher values of $\theta$ or larger values of $\sigma$ allow consumers to reach farther locations, indicating a broader movement range.

Exponential functions are widely employed in ecological modeling to represent resource gradients driven by environmental heterogeneity, owing to their ability to capture nonlinearity and rapid changes in resource availability. For instance, light intensity in aquatic ecosystems attenuates exponentially with depth, as described by the Beer–Lambert law [24]. Similarly, metabolic rates in organisms scale exponentially with temperature, affecting resource productivity across spatial gradients [18]. This pattern extends to processes such as soil nutrient dynamics [22] and plant growth responses [38]. Compared to linear or polynomial models, exponential functions better reflect critical thresholds and abrupt transitions in natural systems [42], making them particularly suited for describing ecological gradients.

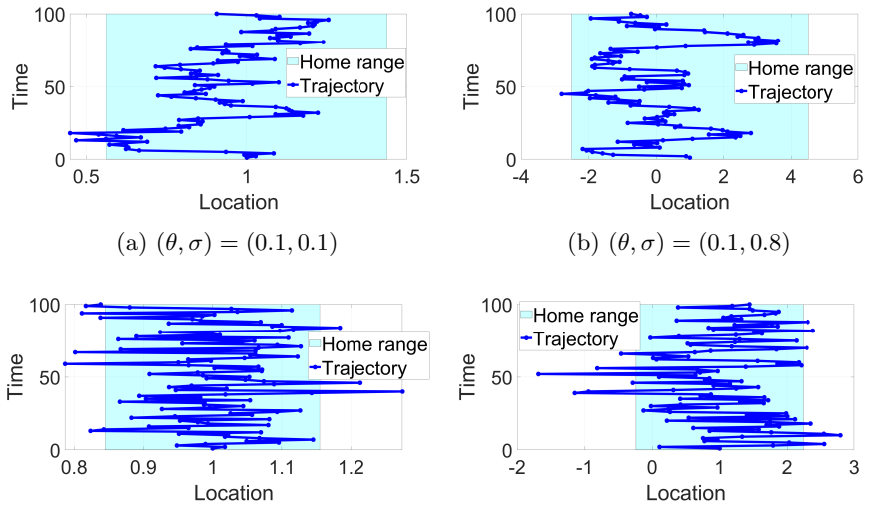


(a) $(\theta, \sigma) = (0.1, 0.1)$ (b) $(\theta, \sigma) = (0.1, 0.8)$

(c) $(\theta, \sigma) = (0.8, 0.1)$ (d) $(\theta, \sigma) = (0.8, 0.8)$

FIG. 1. *Home range and trajectory under varying $\theta$ and $\sigma$ with $\bar{x} = 1$.*

The ecological significance of exponential functions is evident in the relationship between plant growth and spatial temperature gradients. In temperate regions, temperature declines approximately linearly with latitude, where the reference temperature $T_0$ decreases at a rate $c_1$ per degree of latitude $\phi$. According to the Arrhenius equation [25], metabolic processes such as photosynthesis and respiration scale exponentially with temperature, expressed as $R \propto e^{-E_a/(k_B(T_0 - c_1\phi))}$, where $E_a$ is the activation energy and $k_B$ is the Boltzmann constant. This results in a monotonic decline in growth rates with increasing latitude, as seen in the contrast between the rapid growth of tropical rainforests near the equator and the slower rates in boreal forests at higher latitudes [29]. A similar pattern emerges along elevational gradients, where temperature decreases linearly from a reference $T_0$ at a rate $d$ with elevation $h$. Plant growth rates thus decline exponentially, modeled as $R \propto e^{c_2(T_0 - dh)}$, where $c_2$ represents a temperature sensitivity coefficient reflecting the responsiveness of metabolic rates to temperature changes [4]. In the Himalayas, for instance, bamboo forests flourish at lower elevations, while alpine shrubs at higher elevations exhibit significantly reduced growth, aligning with this exponential temperature dependence [48].

Resource heterogeneity in natural systems implies that consumers random spatial movements generate temporal and spatial variability in accessible resources. To explore this, we examine a simplified scenario where environmental factors—such as temperature gradients or light intensity—shape resource availability, resulting in an exponentially monotonic spatial distribution of resources. Consequently, resources available to consumers at varying spatial coordinates are scaled by an exponential factor, modifying interaction terms as follows: $auv \to ae^{cx}uv$ and $abuv \to abe^{cx}uv$, where $c$ governs the rate of exponential change across space.

When $c > 0$, resource availability increases monotonically across space, with greater resources accessible at locations with larger coordinates. Conversely, when $c < 0$, resource availability decreases monotonically, implying higher resource levels at sites with smaller coordinates. If $c = 0$, resources become spatially homogeneous, maintaining constant availability irrespective of location. In this homogeneous

TABLE 1
*Value of parameters in the model* (2.1).

| Paras | Description | Baseline | Range | PRCC |
|---|---|---|---|---|
| $r$ | Intrinsic growth rate | 1 | $[0.8, 1.2]$ | - |
| $k$ | Environmental carrying capacity | 12 | $[9.6, 14.4]$ | 0.1803 |
| $a$ | Consumer consumption rate | 0.08 | $[0.064, 0.096]$ | 0.1748 |
| $b$ | Predation conversion rate | 0.2 | $[0.16, 0.24]$ | 0.1852 |
| $c$ | Impact of the monotonic environment | 0.1 | $[0.01, 2]$ | 0.8854 |
| $m$ | Consumer mortality rate | 0.2 | $[0.16, 0.24]$ | -0.4200 |
| $\bar{x}$ | Home range location | 1.5 | $[0, 2]$ | 0.7588 |
| $\theta$ | Home range attractiveness | 0.3 | $[0.001, 1]$ | -0.4840 |
| $\sigma$ | Stochastic intensity of consumer movement | 0.2 | $[0.001, 1]$ | 0.3200 |

scenario, consumer random spatial movements do not alter resource accessibility, and the long-term consumer dynamics mirror those predicted by the deterministic model [19].

It should be noted, however, that because consumers are constantly moving randomly, resources at each location regenerate quickly after consumption, thereby restoring the original monotonic distribution. This dynamic replenishment maintains the balance in resource availability, allowing the system to retain a stable monotonic distribution despite ongoing consumption. In conclusion, we have developed the following model of consumer random walk under resource monotonic heterogeneity:

(2.1)
$$\begin{cases} \underbrace{\mathrm{d}x(t)}_{\text{Changes in consumer group coordinate}} = \underbrace{\theta}_{\text{attractiveness}} [\underbrace{\bar{x}}_{\text{home location}} - x(t)]\mathrm{d}t + \underbrace{\sigma}_{\text{intensity}} \mathrm{d}B(t), \\ \underbrace{\mathrm{d}u(t)}_{\text{Change in average resource density}} = \left[ \underbrace{ru(t)\left(1 - \frac{u(t)}{k}\right)}_{\text{growth of resource}} - \underbrace{ae^{cx(t)}u(t)v(t)}_{\text{consumed by consumers}} \right] \mathrm{d}t, \\ \underbrace{\mathrm{d}v(t)}_{\text{Change in consumer population}} = \left[ \underbrace{abe^{cx(t)}u(t)v(t)}_{\text{growth of consumer}} - \underbrace{mv(t)}_{\text{death}} \right] \mathrm{d}t. \end{cases}$$

Here, $u$ represents the average resource density across the entire space, and $v$ denotes the total consumer population. The meanings of parameters are provided in Table 1. Next, we proceed to examine the threshold dynamics of the model outlined above and analyze the local probability density function in the vicinity of the positive equilibrium. This investigation will shed light on the conditions necessary for the persistence or extinction of the consumer population and will offer insights into the stability and fluctuations of the population around the equilibrium state.

**3. Threshold dynamics.** To investigate the dynamics of the resource-consumer model (2.1) with stochastic movement, we establish the existence and uniqueness of solution to the following theorem, ensuring the model is well-defined.

THEOREM 3.1. *For any initial value* $(x(0), u(0), v(0)) \in \mathbb{R} \times \mathbb{R}^2_+$*, there exists a unique solution* $(x(t), u(t), v(t))$ *of the model* (2.1) *for* $t \geq 0$*, and this solution will remain in* $\mathbb{R} \times \mathbb{R}^2_+$ *almost surely (a.s.).*

The proof of this theorem is similar to Theorem 3.1 in [57] and will therefore be omitted here.

To determine the long-term behavior of consumers in the stochastic model, we define the stochastic consumption threshold

$$\mathcal{R} = \frac{abke^{c\bar{x}+\frac{c^2\sigma^2}{4\theta}}}{m}.$$

This threshold plays a critical role in deciding whether the consumer population will go extinct or persist over time.

THEOREM 3.2. *If $\mathcal{R} < 1$, then the consumers $v$ in the model* (2.1) *will be extinct exponentially in a long term.*

The proof of the above theorem is presented in Appendix A.1.

For the stochastic model (2.1), the existence of a stationary distribution implies that the consumer population will stabilize over time, indicating long-term persistence of the population.

THEOREM 3.3. *If $\mathcal{R} > 1$, then the stochastic model* (2.1) *admits a stationary distribution.*

The proof of the above theorem is provided in Appendix A.2.

Next, we consider the uniqueness of the stationary distribution within the invariant set of the stochastic model (2.1). An invariant set is a region of the state space where, once the system enters, it remains there for all future times with probability one. For our model, proving the uniqueness of the stationary distribution within this invariant set is crucial for understanding the long-term behavior of the consumer population. Consider

$$\frac{\mathrm{d}}{\mathrm{d}t}\left(u+\frac{v}{b}\right) = -\frac{r}{k}u^2 + (r+m)\,u - m\left(u+\frac{v}{b}\right) \le \frac{k(r+m)^2}{4r} - m\left(u+\frac{v}{b}\right).$$

Hence, the model (2.1) has an invariant set

$$\mathbb{S} = \left\{(x,u,v) \in \mathbb{R}\times\mathbb{R}_+^2 : u + \frac{v}{b} \le \frac{k(r+m)^2}{4mr}\right\}.$$

THEOREM 3.4. *For any initial value $(x(0),u(0),v(0)) \in \mathbb{S}$, the distribution of $(x(t),u(t),v(t))$ has the density $\mathcal{U}(t,x,u,v)$. If $\mathcal{R} > 1$ and $m > r$, there exists the unique density $\mathcal{U}_*(t,x,u,v)$ satisfying*

$$\lim_{t\to\infty}\iiint_{\mathbb{S}} |\mathcal{U}(t,x,u,v) - \mathcal{U}_*(t,x,u,v)|\mathrm{d}x\mathrm{d}u\mathrm{d}v = 0.$$

The proof of the above theorem is provided in Appendix A.3.

To gain a deeper understanding of the stochastic model (2.1), it is essential to examine the local behavior of the system around the quasi-positive equilibrium. The quasi-positive equilibrium represents a critical state where the consumer population remains viable. The local probability density function near this equilibrium provides crucial insights into the likelihood that the system remains close to or deviates from this state under random perturbations. Studying the local probability density function is important for understanding the stability properties of the equilibrium, the frequency and magnitude of fluctuations around it, and the resilience of the consumer population in response to environmental variability. The proof of the theorem is given in Appendix A.4.

THEOREM 3.5. *Assuming that* $abke^{c\bar{x}} > m$, *then the stationary distribution of model* (2.1) *around* $E^* = (\bar{x}, u^*, v^*)$ *approximately obeys* $\mathbb{N}(E^*, \Sigma)$, *where*

$$(u^*, v^*) = \left( \frac{m}{abe^{c\bar{x}}}, \frac{(k-u^*)\,r}{ake^{c\bar{x}}} \right), \quad \Sigma = [\sigma c \bar{\beta} u^* g(v^*)]^2 (T_2 T_1)^{-1} \Omega [(T_2 T_1)^{-1}]^\top,$$

*and*

$$\Omega = \begin{pmatrix} \frac{a_2}{2(a_1 a_2 - a_3)} & 0 & -\frac{1}{2(a_1 a_2 - a_3)} \\ 0 & \frac{1}{2(a_1 a_2 - a_3)} & 0 \\ -\frac{1}{2(a_1 a_2 - a_3)} & 0 & \frac{a_1}{2a_3(a_1 a_2 - a_3)} \end{pmatrix}, \quad T_1 = \begin{pmatrix} 1 & 0 & 0 \\ 0 & 1 & 0 \\ 0 & b & 1 \end{pmatrix},$$

$$T_2 = \begin{pmatrix} ace^{c\bar{x}} u^* v^* a_4 & -\frac{ru^*}{k} a_4 & ae^{c\bar{x}} u^* \left( \frac{bru^*}{k} - abe^{c\bar{x}} v^* \right) \\ 0 & a_4 & -abe^{c\bar{x}} u^* \\ 0 & 0 & 1 \end{pmatrix},$$

*with* $a_1 = \theta + \frac{ru^*}{k}$, $a_2 = \frac{\theta r u^*}{k} + a^2 b e^{2c\bar{x}} u^* v^*$, $a_3 = a^2 b \theta e^{2c\bar{x}} u^* v^*$, $a_4 = b(abe^{c\bar{x}} u^* + ae^{c\bar{x}} v^* - \frac{r}{k} u^*)$.

**4. Numerical simulation.** In this section, we conduct numerical simulations on model (2.1) to explore how random consumer movements affect the dynamics of the resource-consumer model. Some parameters of the model are derived from [55], while the rest are assumed. Specifically, we simulate various scenarios to analyze the sensitivity of the model parameters in Table 1 to the stochastic consumption threshold $\mathcal{R}$, the dynamics of this threshold, the local probability density near the quasi-equilibrium $E^*$, and the optimal home location for the consumer group. Through these simulations, we aim to determine how random movement patterns and threshold behaviors affect the interactions between resources and consumers.

**4.1. Sensitivity analysis.** We perform a sensitivity analysis by calculating the partial rank correlation coefficients (PRCC) related to the stochastic consumption threshold $\mathcal{R}$ to evaluate the influence of different parameters [49], as illustrated in Figure 2 and Table 1. The results show that the effects of environmental monotonicity $c$, consumer home location $\bar{x}$, home attractiveness $\theta$, intensity of random walk $\sigma$, and consumer mortality rate $m$ have relatively high sensitivity indices. In the next

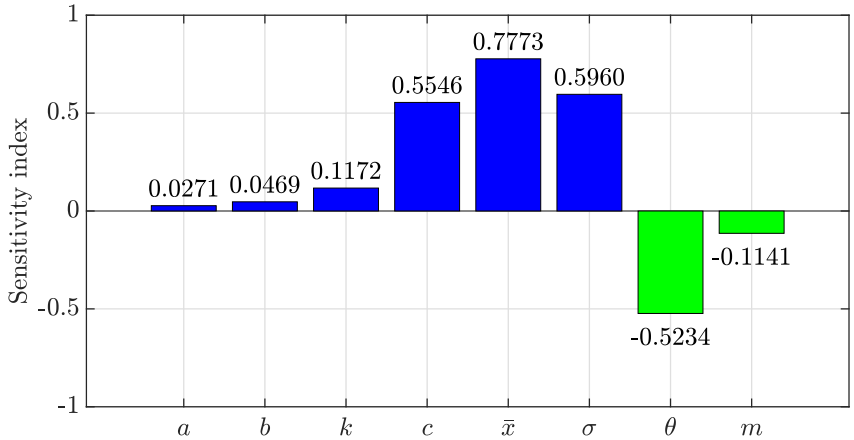


FIG. 2. *PRCC sensitivity analysis for the stochastic consumption threshold* $\mathcal{R}$.

subsection, we will further simulate how these parameter values affect the threshold dynamics of the stochastic model (2.1).

**4.2. Threshold dynamics.** In this section, we begin by presenting the discretized form of the model (2.1) using the Euler–Maruyama method [21]:

$$\begin{cases} x_{i+1} = x_i + \theta(\bar{x} - x_i)\Delta t + \sigma\xi_i\sqrt{\Delta t}, \\ u_{i+1} = u_i + \left[ru_i\left(1 - \dfrac{u_i}{k}\right) - ae^{cx_i}u_iv_i\right]\Delta t, \\ v_{i+1} = v_i + \left[abe^{cx_i}u_iv_i - mv_i\right]\Delta t, \end{cases} \tag{4.1}$$

where $(x_i, u_i, v_i)$ represents the value at the $i$th iteration of the discretization equation; $\Delta t$ is the time increment; $\xi_i$ are mutually independent Gaussian random variables following the standard normal distribution for $i = 1, 2, \ldots, n$; and the initial value $(x(0), S(0), I(0)) = (\bar{x}, 10, 0.1)$. This numerical scheme enables us to approximate the SDE and examine its dynamic behavior under different conditions.

To examine the factors influencing the persistence or extinction of consumer populations in stochastic environments, we focus on five key parameters that influence the dynamics of the resource-consumer model:

- Environmental monotonicity ($c$) is crucial in determining resource availability within the consumer's home range. A higher $c$ results in a more consistent increase in resources near the consumer's home, thereby enhancing survival chances by providing steady access to essential nutrients. In contrast, lower $c$ reduces resource availability, potentially pushing the consumer population toward extinction. Figure 3(a) illustrates the results.
- Home location ($\bar{x}$) significantly affects consumer survival by determining access to resources. Settling in areas with higher resource density allows consumers to optimize their resource intake, enhancing overall fitness and growth rates. Conversely, settling in less favorable locations with lower resource density may limit access to necessary nutrients, resulting in population decline. Figure 3(b) shows the results.
- Home attractiveness ($\theta$) determines the tendency of consumers to remain within their home range or disperse to other areas. A lower home attractiveness facilitates movement toward regions with higher resource availability, improving foraging efficiency and adaptability to changing resource landscapes. In contrast, excessive home attractiveness can trap consumers in less favorable areas, restricting their ability to explore and exploit richer resource patches, thereby reducing their overall fitness. The results are given in Figure 3(c).
- Random walk intensity ($\sigma$) influences the ability of consumers to find and utilize resource-rich patches. A high level of random walk intensity allows consumers to explore a broader area, increasing their chances of locating resources. However, if the movement intensity is too low, consumers may fail to reach areas with high resource density, limiting their net energy intake and reducing their survival likelihood. The results are presented in Figure 3(d).
- Mortality rate ($m$) directly influences the survival prospects of consumer population. A lower mortality rate reduces the baseline risk of death, allowing the population to persist longer under various environmental conditions. In contrast, a higher mortality rate increases the likelihood of extinction. Figure 3(e) demonstrates the results.

Furthermore, we investigate the fluctuation characteristics of the persistent consumer population (represented by the blue curve) in Figures 3(c) and 3(d).

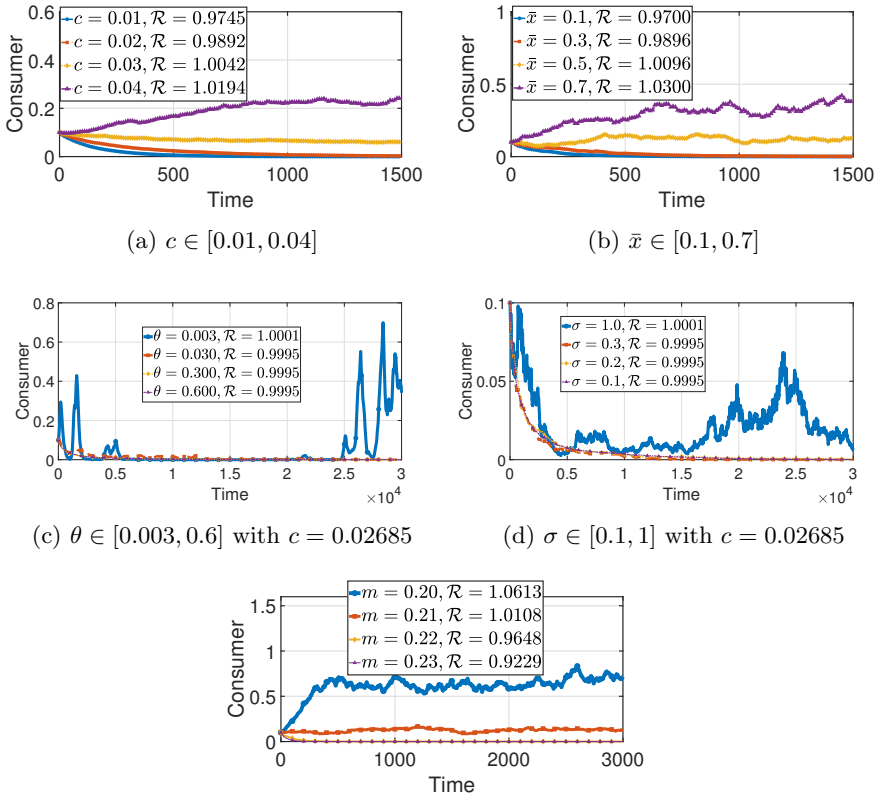


(a) $c \in [0.01, 0.04]$

(b) $\bar{x} \in [0.1, 0.7]$

(c) $\theta \in [0.003, 0.6]$ with $c = 0.02685$

(d) $\sigma \in [0.1, 1]$ with $c = 0.02685$

(e) $m \in [0.2, 0.23]$.

FIG. 3. *Relationship between consumer population size and different parameters.*

Our analysis reveals that while the location of the consumer population follows a normal distribution, $x \sim \mathbb{N}(\frac{3}{2}, \frac{1}{60})$, the population sizes display strikingly different behaviors. To elucidate how movement within the same home range can lead to varying degrees of fluctuation in consumer numbers, we introduce Figure 4, which depicts the temporal evolution of both the consumer population size and its spatial position for the persistent states shown in Figures 3(c) and 3(d).

In Figure 4(a), where $\theta = 0.003$, the home attractiveness is relatively weak. This reduced attractiveness results in a lower frequency of returns to the home location. Consequently, consumers tend to spend extended periods in regions with either low or high resource availability. This prolonged residence in areas of varying resource levels can trigger oscillations in population density, resembling the predator-prey cycles observed in spatially explicit ecological models [26]. The slower movement and extended linger time amplify these fluctuations.

In contrast, Figure 4(b) illustrates a scenario with a larger $\theta$, corresponding to stronger home attractiveness. This increases the frequency of returns to the home location, enabling consumers to move more rapidly between resource patches. As a result, the population experiences less severe fluctuations, as the frequent movement smooths out the effects of spatial resource variation.

This observation is consistent with ecological studies on animal movement, which suggest that the balance between home range size and return frequency plays a key

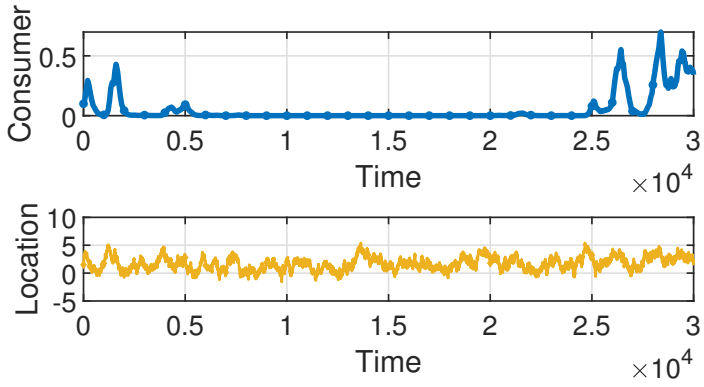


(a) $\theta = 0.003$, $\sigma = 0.1$ and $c = 0.02685$ with $\mathcal{R} = 1.0001$

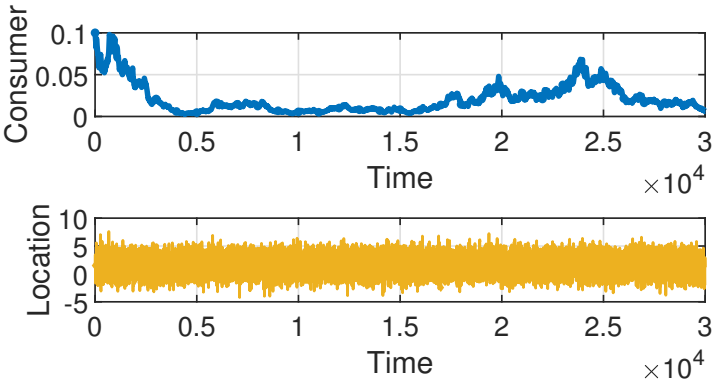


(b) $\theta = 0.3$, $\sigma = 1$ and $c = 0.02685$ with $\mathcal{R} = 1.0001$

FIG. 4. *Fluctuations in the number and position of consumer populations.*

role in regulating population stability [30]. In stochastic or spatially heterogeneous environments, these factors emerge as critical determinants of resource-consumer dynamics.

**4.3. Mean extinction time.** To further examine the impact of the parameters discussed above on consumer extinction, we focus on the mean extinction time (MET) for different parameter values when $\mathcal{R} < 1$. The MET offers a quantitative measure of the average time required for the consumer population to reach extinction from an initial state under different conditions.

Define the extinction time from the initial state $(x(0), u(0), v(0)) = (\bar{x}, 10, 0.1)$ to the extinct state as

$$\tau = \inf\{t : v(t) < 10^{-4}\}.$$

Here, $v(t)$ represents the consumer population at time $t$. The extinction time $\tau$ is defined as the first time when the consumer density $v(t)$ falls below the threshold value of $10^{-4}$. This consumption threshold indicates that the consumer population is effectively extinct, as the density has become negligibly small. Taking an average over the extinction time yields

$$\mathrm{MET} = \mathbb{E}(\tau).$$

The MET is the expected value of the extinction time $\tau$, which reflects the average duration until extinction across many simulations. To compute the MET, we perform a large number of simulations under different parameter settings. Applying the Euler–Maruyama method for numerical simulation, in this context, if $v(n\Delta t) < 10^{-4}$, then the extinction time $\tau = n\Delta t$, where $n$ represents the discrete time step and $\Delta t$ is the time increment. The MET can then be calculated as $\mathrm{MET} = \frac{1}{N}\sum_{i=1}^{N} n_i \Delta t$, where $N$ is the total number of simulations performed, and $n_i$ represents the discrete time step at which the extinction condition $v(n_i\Delta t) < 10^{-4}$ is first met in the $i$th simulation. For the numerical simulations, we choose $N = 10^4$.

Figure 5 shows that the MET is influenced by various parameter values: a decrease in environmental monotonicity ($c$), home location ($\bar{x}$), and random walk intensity ($\sigma$) all lead to a shorter MET, as these conditions limit access to resources and reduce the ability to explore or settle in areas with higher resource density. Conversely, an increase in home attractiveness ($\theta$) and mortality rate ($m$) also reduces the MET, as higher $\theta$ confines movement to less favorable areas, while a higher $m$ directly increases the risk of death. Together, these factors demonstrate that changes in any of these parameters can significantly shorten the time until extinction in stochastic environments.

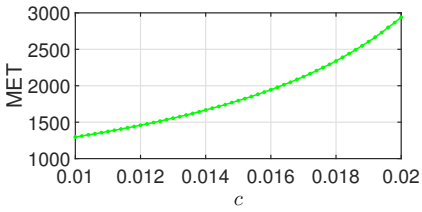


(a) $c \in [0.01, 0.02]$.

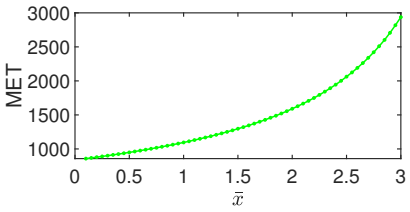


(b) $\bar{x} \in [0.1, 3]$.

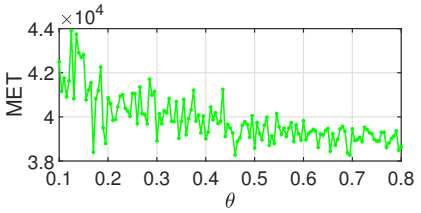


(c) $\theta \in [0.1, 0.8]$ with $c = 0.02685$.

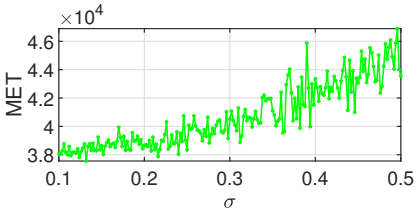


(d) $\sigma \in [0.1, 0.5]$ $c = 0.02685$.

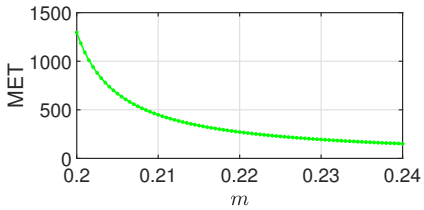


(e) $m \in [0.2, 0.24]$.

FIG. 5. *Relationship between mean extinction time and different parameters.*

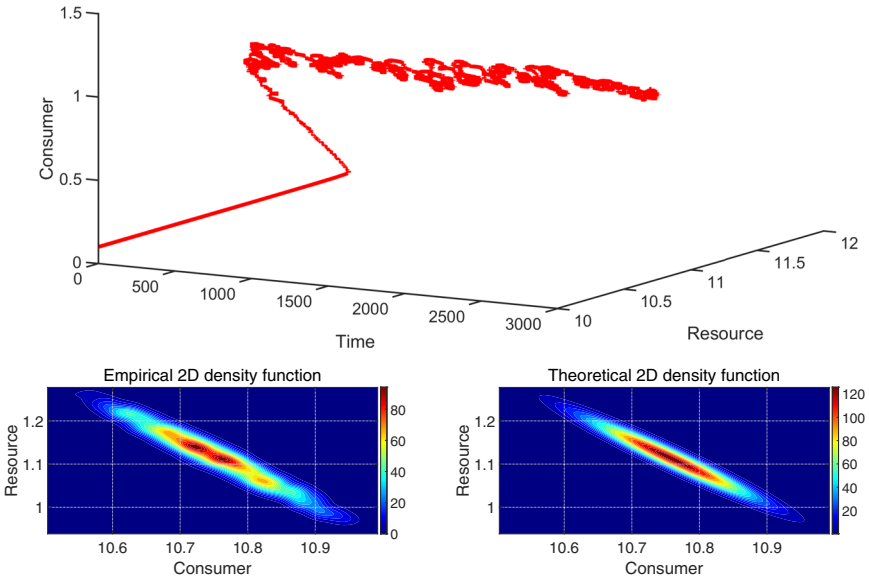


FIG. 6. *The top panel shows a 3D phase plot of resources and consumers for* $t \in (0, 3000)$. *The bottom left panel displays the empirical probability density function of resources and consumers for* $t \in (300, 3000)$, *while the bottom right panel shows the theoretically calculated local probability density function.*

**4.4. Local density function.** Based on the parameters in Table 1, it is calculated that $abke^{\bar{x}} = 0.2231$. From the expression in Theorem 3.5, we obtain the local probability density function around E * obeys $\mathbb{N}_3(E^*, \Sigma)$, where

$$E^* = (1.5, 10.7588, 1.1128),\ \Sigma = \begin{pmatrix} 0.06667 & -0.009770 & 0.004272 \\ -0.009770 & 0.006339 & -0.004596 \\ 0.004272 & -0.004596 & 0.003559 \end{pmatrix}.$$

Additionally, from the expression for the probability density function, we can deduce that $(u, v)$ follows a bivariate normal distribution

$$(u, v) \sim \mathbb{N}\left((10.7588, 1.1128), \begin{pmatrix} 0.006339 & -0.004596 \\ -0.004596 & 0.003559 \end{pmatrix}\right),$$

which is shown in Figure 6. Specifically, one obtains $u \sim \mathbb{N}(10.7588, 0.006339)$ and $v \sim \mathbb{N}(1.1128, 0.003559)$ (see Figure 7).

**4.5. Optimal home location for consumers.** In Figure 8, the optimal home location for consumers is $\bar{x} = 7.4$, rather than a very large positive value of $\bar{x}$. Theorem 3.5 defines the long-term averages of the consumer density $v^*$, with the derivative

$$\frac{\partial v^*}{\partial \bar{x}} = \frac{r(abke^{c\bar{x}} - m)}{a^2 bke^{2c\bar{x}}},$$

indicating that $v^*$ takes the maximum value at $\bar{x} = \frac{1}{c}\ln(\frac{2m}{abk}) \approx 7.4$ for $c = 0.1$.

Simulations reveal that for $\bar{x} \in (-\infty, 0.4)$, the stochastic consumption threshold $\mathcal{R} < 1$, suggesting consumer extinction due to insufficient resource utilization. Conversely, for $\bar{x} \in (0.4, +\infty)$, $\mathcal{R} > 1$, indicating persistence. Despite the unrestricted settlement range $(-\infty, +\infty)$ and rising resource availability providing more resources at

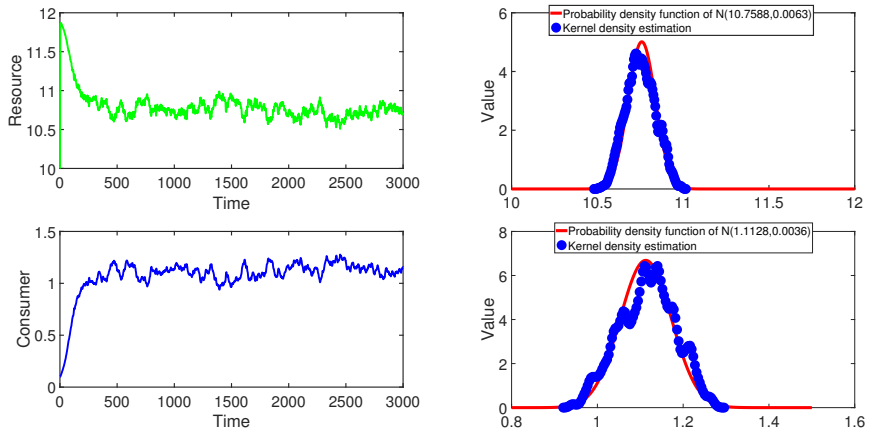


FIG. 7. *The left panel shows the trajectory of resource density (green line) and consumer quantity (blue line) for* $t \in (0, 3000)$. *The right panel displays the empirical density fitting points (blue dots) for* $t \in (300, 3000)$ *along with the theoretically calculated marginal probability density function (red line).*

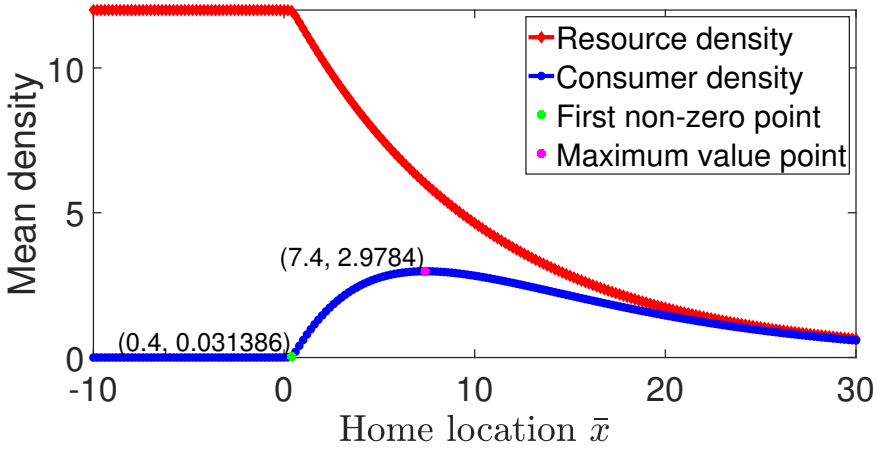


FIG. 8. *Impact of home location* $\bar{x}$ *on the average resource and consumer density under* $t = 3000$.

larger $\bar{x}$, excessive consumer density at high $\bar{x}$ depletes the long-term resource density $u$, reducing available resources and subsequently consumer numbers. Consequently, as $\bar{x}$ increases, the long-term consumer density initially rises and then declines, establishing $\bar{x} = \frac{1}{c}\ln(\frac{2m}{abk})$ as the optimal home location. This reflects an equilibrium between resource use and population dynamics.

**5. Discussion.** In this study, we developed an integrated model that combines stochastic consumer movement, specifically utilizing the OU process, with resource-consumer dynamics in spatially heterogeneous environments. By incorporating random walk behavior and variability in resource availability across locations, the model provides a more realistic representation of ecological processes, capturing the complex interactions between consumer movements and resource dynamics. Our findings show that consumer movement within a home range, shaped by environmental factors and individual decision making, plays a crucial role in population stability and species

coexistence. This underscores the importance of including stochastic elements in ecological models to improve our understanding and predictions of population dynamics.

The integration of stochastic movement into resource-consumer models marks a significant advancement in modeling ecological dynamics in heterogeneous landscapes. Traditional deterministic models often overlook the randomness and adaptability of consumer behavior in real world environments. Using the OU process for random walks, our model addresses these gaps, offering a framework to explore how consumers navigate complex resource distributions, respond to environmental fluctuations, and adjust their survival and reproduction strategies.

This study holds both theoretical and practical significance. Theoretically, it emphasizes the necessity of incorporating spatial heterogeneity and stochastic consumer movement into models to better reflect the adaptive strategies of populations. It sheds light on key processes such as population persistence and random walks within home ranges, providing deeper insight into the dynamic interactions between resources and consumers. Practically, our model offers a valuable tool for resource management and optimizing consumer home ranges, particularly under changing environmental conditions.

However, several areas warrant further investigation. Future research could explore more complex movement patterns, such as those influenced by social interactions, learning, or memory [54, 51, 45], which were not included in this model. Empirical validation using field data is also crucial to test the applicability across different ecosystems [8, 14]. Further development could incorporate multi-species interactions to better understand coexistence and competition under varying environmental conditions. In general, this study lays the foundation for a more nuanced understanding of consumer-resource dynamics, paving the way for more effective ecological management and conservation strategies.

## Appendix A. Proof of Theorems.

### A.1. Proof of Theorem 3.2.

LEMMA A.1 (see [46]). *For an SDE,*

$$\mathrm{d}\mathcal{X}(t) = \theta(\bar{\mathcal{X}} - \mathcal{X}(t)) + \sigma B(t),$$

*where $\theta$, $\bar{\mathcal{X}}$, and $\sigma$ are positive constants and $B(t)$ is a standard Brownian motion. For any $n > 0$, then*

$$\lim_{t\to\infty} \frac{1}{t} \int_0^t e^{n\mathcal{X}(s)} \mathrm{d}s = e^{n\bar{\mathcal{X}} + \frac{n^2\sigma^2}{4\theta}}.$$

*Proof.* Consider the following one-dimensional differential equation:

$$\frac{\mathrm{d}U(t)}{\mathrm{d}t} = rU(t)\left(1 - \frac{U(t)}{k}\right). \tag{A.1}$$

Assume that $U(t)$ is the solution to model (A.1) with $U(0) = u(0)$: according to the comparison theorem of one-dimensional SDE [36], it follows that $u(t) \le U(t)$. Applying Itô's formula to $W_2 = U - k - k\ln\frac{U}{k}$, then we have

$$\mathcal{L}W_2 = \left(1 - \frac{k}{U}\right)\left(rU - \frac{r}{k}U^2\right) = -\frac{r}{k}(U-k)^2. \tag{A.2}$$

Integrating (A.2) from 0 to $t$ and dividing by $t$ on both sides, we have

$$\frac{W_2(t)-W_2(0)}{t} \le \frac{1}{t}\int_0^t -\frac{r}{k}(U(s)-k)^2 \mathrm{d}s. \tag{A.3}$$

As $t\to\infty$, it can be obtained that

$$\limsup_{t\to\infty}\frac{1}{t}\int_0^t (U(s)-k)^2\mathrm{d}s \le \limsup_{t\to\infty}\frac{k(W_2(t)-W_2(0))}{rt}=0. \tag{A.4}$$

Based on Young's inequality, for a positive constant $\rho_1$, we have

$$e^{cx}|U-K| \le \frac{e^{2cx}}{4\rho_1}+\rho_1|U-K|^2. \tag{A.5}$$

Applying Itô's formula to $\ln v$ and combining (A.5), we have

$$\begin{aligned}\mathcal{L}(\ln v) &= abe^{cx}u - m \le abe^{cx}U - m = e^{cx}abk - m + e^{cx}(U-k)\\ &\le e^{cx}abk - m + \frac{e^{2cx}}{4\rho_1}+\rho_1|U-k|^2.\end{aligned} \tag{A.6}$$

Integrating (A.6) from 0 to $t$ and dividing by $t$ on both sides, we have

$$\begin{aligned}\frac{\ln v(t)-\ln v(0)}{t} \le{}& \frac{abk}{t}\int_0^t e^{cx(s)}\mathrm{d}s - m + \frac{1}{4\rho_1 t}\int_0^t e^{2cx(s)}\mathrm{d}s\\ &+\frac{\rho_1}{t}\int_0^t |U(s)-k|^2\mathrm{d}s, \text{ a.s.}\end{aligned} \tag{A.7}$$

According to Lemma A.1, one gets

$$\lim_{t\to\infty}\frac{1}{t}\int_0^t e^{cx(s)}\mathrm{d}s = e^{c\bar{x}+\frac{c^2\sigma^2}{4\theta}},\ \lim_{t\to\infty}\frac{1}{t}\int_0^t e^{2cx(s)}\mathrm{d}s = e^{2c\bar{x}+\frac{c^2\sigma^2}{\theta}}. \tag{A.8}$$

Choose $\rho_1 = \frac{e^{2c\bar{x}+\frac{c^2\sigma^2}{\theta}}}{2m(1-\mathcal{R})}$ such that

$$\frac{e^{2c\bar{x}+\frac{c^2\sigma^2}{\theta}}}{4\rho_1} = \frac{m}{2}(1-\mathcal{R}). \tag{A.9}$$

Taking the superior limit of $t$ on both sides of (A.7) and then combining (A.4), (A.8), and (A.9), we have

$$\limsup_{t\to\infty}\frac{\ln v(t)}{t} \le abke^{c\bar{x}+\frac{c^2\sigma^2}{4\theta}} - m + \frac{m}{2}(1-\mathcal{R}) = \frac{m}{2}(\mathcal{R}-1) < 0, \quad \text{a.s.}$$

The proof is completed. ∎

### A.2. Proof of Theorem 3.3.

*Proof.* First, making the use of Itô's formula to $-\ln v$ and $u-k-\ln\frac{u}{k}$, respectively, we have

$$\begin{aligned}\mathcal{L}(-\ln v) &= -e^{cx}qu + m\\ &= -e^{cx}abk + m + abe^{cx}(k-u)\\ &\le -e^{cx}abk + m + abe^{cx}|k-u|\\ &\le -e^{cx}abk + m + ab\left(\frac{e^{2cx}}{4\rho_2}+\rho_2(k-u)^2\right),\end{aligned} \tag{A.10}$$

where $\rho_2$ is a positive constant to be determined later, and

$$\begin{aligned}\mathcal{L}\left(u-k-k\ln\frac{u}{k}\right)&=\left(1-\frac{k}{u}\right)\left[ru\left(1-\frac{u}{k}\right)-e^{cx}auv\right]\\&=-\frac{r}{k}(k-u)^2-e^{cx}auv+ake^{cx}v\\&\le-\frac{r}{k}(k-u)^2+ake^{cx}v.\end{aligned}\tag{A.11}$$

Define

$$W_3=-\ln v+\frac{k(ab\rho_2+\rho_3)}{r}\left(u-k-\ln\frac{u}{k}\right),$$

where $\rho_2$ and $\rho_3$ are positive constants to be determined later. Combining (A.10) and (A.11), we obtain

(A.12)

$$\begin{aligned}\mathcal{L}W_3\le&-abke^{cx}+m-\rho_3(k-u)^2+\frac{abe^{2cx}}{4\rho_2}+\frac{ak^2(ab\rho_2+\rho_3)}{r}e^{cx}v\\\le&-abke^{cx}+m-\rho_3(k-u)^2+\frac{abe^{2cx}}{4\rho_2}+\frac{ak^2(ab\rho_2+\rho_3)}{r}\left(\rho_4e^{2cx}+\frac{v^2}{4\rho_4}\right)\\=&-m(\mathcal{R}-1)-\rho_3(k-u)^2+\left(\frac{ab}{4\rho_2}+\frac{ak^2\rho_4(ab\rho_2+\rho_3)}{r}\right)e^{2c\bar{x}+\frac{c^2\sigma^2}{\theta}}\\&+\frac{a^2bk^2\rho_2}{4r\rho_4}v^2+p_2(x),\end{aligned}$$

where $\rho_4$ is determined in (A.13) and

$$p_2(x)=abk\left(e^{c\bar{x}+\frac{c^2\sigma^2}{4\theta}}-e^{cx}\right)+\left(\frac{ab}{4\rho_2}+\frac{ak^2\rho_4(ab\rho_2+\rho_3)}{r}\right)\left(e^{2c\bar{x}+\frac{c^2\sigma^2}{\theta}}-e^{2cx}\right).$$

Choose

$$\rho_2=\frac{ab}{m(\mathcal{R}-1)e^{2c\bar{x}+\frac{c^2\sigma^2}{\theta}}},\ \rho_4=\frac{rm(\mathcal{R}-1)}{4ak^2\rho_4(ab\rho_2+\rho_3)e^{2c\bar{x}+\frac{c^2\sigma^2}{\theta}}}.\tag{A.13}$$

Then (A.12) leads to

$$\mathcal{L}W_3\le-\frac{m(\mathcal{R}-1)}{2}-\rho_3(k-u)^2+\frac{a^2bk^2\rho_2}{4r\rho_4}v^2+p_2(x).\tag{A.14}$$

Define $W_4=(e^x-x-1)+\frac{1}{3}(u+\frac{v}{b})^3$. Applying Itô's formula to $W_4$, we have

(A.15)

$$\begin{aligned}\mathcal{L}W_4=&\theta(\bar{x}-x)(e^x-1)+\frac{\sigma^2}{2}e^x+\left(u+\frac{v}{b}\right)^2\left(ru\left(1-\frac{u}{k}\right)-\frac{m}{b}v\right)\\\le&\theta(\bar{x}-x)(e^x-1)+\frac{\sigma^2}{2}e^x-\frac{r}{k}u^4-\frac{m}{b^3}v^3-\frac{r}{b^2k}u^2v^2+ru^3+\frac{r}{b^2}uv^2+\frac{2r}{b}u^2v\\\le&\theta(\bar{x}-x)(e^x-1)+\frac{\sigma^2}{2}e^x-\frac{r}{2k}u^4-\frac{m}{2b^3}v^3+\rho_5,\end{aligned}$$

where $\rho_5=\sup_{(u,v)\in\mathbb{R}^2_+}\{-\frac{r}{2k}u^4-\frac{m}{2b^3}v^3-\frac{r}{b^2k}u^2v^2+ru^3+\frac{r}{b^2}uv^2+\frac{2r}{b}u^2v\}$. Then we define $W_5=\rho_6W_3+W_4$, where $\rho_6$ is a sufficiently large constant satisfying

$$-\frac{\rho_6m(\mathcal{R}-1)}{2}+\rho_5+\sup_{x\in\mathbb{R}}\left\{\theta(\bar{x}-x)(e^x-1)+\frac{\sigma^2}{2}e^x\right\}\le-2.\tag{A.16}$$

From (A.14) and (A.15), we have $\mathcal{L}W_5 \le g(x,u,v) + \rho_6 p_2(x)$, where

$$g(x,u,v) = -\frac{\rho_6 m(\mathcal{R}-1)}{2} - \rho_3\rho_6(k-u)^2 + \frac{a^2bk^2\rho_2\rho_6}{4r\rho_4}v^2 + \theta(\bar{x}-x)(e^x-1) + \frac{\sigma^2}{2}e^x - \frac{r}{2k}u^4 - \frac{m}{2b^3}v^3 + \rho_5. \tag{A.17}$$

Construct a compact set

$$\mathbb{D} = \left\{(x,u,v) \in \mathbb{R}\times\mathbb{R}_+^2 : |x| \le \frac{1}{\kappa}, \kappa \le u \le \frac{1}{\kappa}, \kappa \le v \le \frac{1}{\kappa}\right\}$$

such that $g(x,u,v) \le -1$ for any $(x,u,v) \in \mathbb{R}\times\mathbb{R}_+^2 \setminus \mathbb{D} := \mathbb{D}^c$. Then let $\mathbb{D}^c = \bigcup_{i=1}^6 \mathbb{D}_i^c$, where

$$\mathbb{D}_1^c = \left\{(x,u,v) \in \mathbb{R}\times\mathbb{R}_+^2 : x > \frac{1}{\kappa}\right\}, \qquad \mathbb{D}_2^c = \left\{(x,u,v) \in \mathbb{R}\times\mathbb{R}_+^2 : x < -\frac{1}{\kappa}\right\},$$
$$\mathbb{D}_3^c = \{(x,u,v) \in \mathbb{R}\times\mathbb{R}_+^2 : v < \kappa\}, \qquad \mathbb{D}_4^c = \left\{(x,u,v) \in \mathbb{R}\times\mathbb{R}_+^2 : v > \frac{1}{\kappa}\right\},$$
$$\mathbb{D}_5^c = \left\{(x,u,v) \in \mathbb{R}\times\mathbb{R}_+^2 : v \le \frac{1}{\kappa}, u < \kappa\right\}, \quad \mathbb{D}_6^c = \left\{(x,u,v) \in \mathbb{R}\times\mathbb{R}_+^2 : u > \frac{1}{\kappa}\right\},$$

with $\kappa$ being a small enough constant satisfying

$$\min\left\{-\frac{\theta}{2\kappa}e^{\frac{1}{\kappa}}, -\frac{\theta}{2\kappa}(1-e^{-\frac{1}{\kappa}})\right\} + \sup_{x\in\mathbb{R}}\left\{\theta\left(\bar{x}-\frac{x}{2}\right)(e^x-1) + \frac{\sigma^2}{2}e^x\right\} + \sup_{v\in\mathbb{R}_+}\left\{\frac{a^2bk^2\rho_2\rho_6}{4r\rho_4}v^2 - \frac{m}{2b^3}v^3\right\} + \rho_5 \le -1; \tag{A.18}$$

$$\frac{a^2bk^2\rho_2\rho_6}{4r\rho_4}\kappa^2 \le 1; \tag{A.19}$$

$$\min\left\{-\frac{m}{4b^3\kappa^3}, -\frac{r}{2k\kappa^4}\right\} + \sup_{v\in\mathbb{R}_+}\left\{\frac{a^2bk^2\rho_2\rho_6}{4r\rho_4}v^2 - \frac{m}{4b^3}v^3\right\} \le 1. \tag{A.20}$$

If $(x,u,v) \in \mathbb{D}_1^c$, from (A.17) and (A.18), we have

$$\begin{aligned} g(x,u,v) &\le \theta(\bar{x}-x)(e^x-1) + \frac{\sigma^2}{2}e^x + \frac{a^2bk^2\rho_2\rho_6}{4r\rho_4}v^2 - \frac{m}{2b^3}v^3 + \rho_5 \\ &\le -\frac{\theta}{2\kappa}e^{\frac{1}{\kappa}} + \sup_{x\in\mathbb{R}}\left\{\theta\left(\bar{x}-\frac{x}{2}\right)(e^x-1) + \frac{\sigma^2}{2}e^x\right\} \\ &\quad + \sup_{v\in\mathbb{R}_+}\left\{\frac{a^2bk^2\rho_2\rho_6}{4r\rho_4}v^2 - \frac{m}{2b^3}v^3\right\} + \rho_5 \\ &\le -1. \end{aligned}$$

If $(x,u,v) \in \mathbb{D}_2^c$, from (A.17) and (A.18), we obtain

$$\begin{aligned} g(x,u,v) &\le \theta(\bar{x}-x)(e^x-1) + \frac{\sigma^2}{2}e^x + \frac{a^2bk^2\rho_2\rho_6}{4r\rho_4}v^2 - \frac{m}{2b^3}v^3 + \rho_5 \\ &\le -\frac{\theta}{2\kappa}(1-e^{-\frac{1}{\kappa}}) + \sup_{x\in\mathbb{R}}\left\{\theta\left(\bar{x}-\frac{x}{2}\right)(e^x-1) + \frac{\sigma^2}{2}e^x\right\} \\ &\quad + \sup_{v\in\mathbb{R}_+}\left\{\frac{a^2bk^2\rho_2\rho_6}{4r\rho_4}v^2 - \frac{m}{2b^3}v^3\right\} + \rho_5 \\ &\le -1. \end{aligned}$$

If $(x,u,v)\in\mathbb{D}_3^c$, from (A.16), (A.17), and (A.19), one has

$$g(x,u,v)\le\frac{a^2bk^2\rho_2\rho_6}{4r\rho_4}v^2-2\le\frac{a^2bk^2\rho_2\rho_6}{4r\rho_4}\kappa^2-2\le-1.$$

If $(x,u,v)\in\mathbb{D}_4^c$, from (A.16), (A.17), and (A.20), one gets

$$\begin{aligned}g(x,u,v)\le&\frac{a^2bk^2\rho_2\rho_6}{4r\rho_4}v^2-2-\frac{m}{2b^3}v^3\\ \le&-\frac{m}{4b^3}v^3+\sup_{v\in\mathbb{R}_+}\left\{\frac{a^2bk^2\rho_2\rho_6}{4r\rho_4}v^2-\frac{m}{4b^3}v^3\right\}-2\\ \le&-\frac{m}{4b^3\kappa^3}+\sup_{v\in\mathbb{R}_+}\left\{\frac{a^2bk^2\rho_2\rho_6}{4r\rho_4}v^2-\frac{m}{4b^3}v^3\right\}-2\\ \le&-1.\end{aligned}$$

If $(x,u,v)\in\mathbb{D}_5^c$, from (A.16), and (A.17), we have

$$\begin{aligned}g(x,u,v)\le&-\rho_3\rho_6(k-u)^2+\frac{a^2bk^2\rho_2\rho_6}{4r\rho_4}v^2-2\le-\frac{\rho_3\rho_6(k-\kappa)^2}{4}\\ &+\frac{a^2bk^2\rho_2\rho_6}{4r\rho_4\kappa^2}-2\le-1,\end{aligned}$$

where letting $\rho_3=\frac{a^2bk^2\rho_2}{r\rho_4(k-\kappa)^2}$ makes the last inequality hold.

If $(x,u,v)\in\mathbb{D}_6^c$, from (A.16), (A.17), and (A.20), one has

$$\begin{aligned}g(x,u,v)\le&\frac{a^2bk^2\rho_2\rho_6}{4r\rho_4}v^2-\frac{r}{2k}u^4-\frac{m}{2b^3}v^3-2\\ \le&-\frac{r}{2k\kappa^4}+\sup_{v\in\mathbb{R}_+}\left\{\frac{a^2bk^2\rho_2\rho_6}{4r\rho_4}v^2-\frac{m}{2b^3}v^3\right\}-2\\ \le&-1.\end{aligned}$$

In summary, we have $g(x,u,v)\le-1$ for any $(x,u,v)\in\mathbb{D}^c$. Then it can be found that the function $g(x,u,v)$ tends to $\infty$ when $u$ or $v$ approaches the boundary of $\mathbb{R}_+$ or when $x\to\pm\infty$. Thus, there exists a point $(\underline{x},\underline{u},\underline{v})$ in the interior of $\mathbb{R}\times\mathbb{R}_+^2$ such that $g(\underline{x},\underline{u},\underline{v})$ takes the minimum value. Thus, $W_5(x,u,v)=W_4(x,u,v)-W_4(\underline{x},\underline{u},\underline{v})$ is a nonnegative $C^2$-function. Applying Itô's formula to $W_5(x,u,v)$, we obtain

$$\mathcal{L}W_5(x,u,v)\le g(x,u,v)+\rho_6p_2(x).$$

For any initial value $(x(0),u(0),v(0))\in\mathbb{R}\times\mathbb{R}_+^2$ and the time interval $[0,t]$, we have

$$\begin{aligned}0\le&\frac{\mathbb{E}W_5(x(t),u(t),v(t))}{t}\\ \le&\frac{\mathbb{E}W_5(x(0),u(0),v(0))}{t}+\frac{1}{t}\int_0^t\mathbb{E}(g(x(\tau),u(\tau),v(\tau)))\mathrm{d}\tau\\ &+abk\left(e^{c\bar{x}+\frac{c^2\sigma^2}{4\theta}}-\mathbb{E}\left(\frac{1}{t}\int_0^te^{cx(\tau)}\mathrm{d}\tau\right)\right)\\ &+\left(\frac{ab}{4\rho_2}+\frac{ak^2\rho_4(ab\rho_2+\rho_3)}{r}\right)\left(e^{2c\bar{x}+\frac{c^2\sigma^2}{\theta}}-\left(\frac{1}{t}\int_0^te^{2cx(\tau)}\mathrm{d}\tau\right)\right).\end{aligned}\tag{A.21}$$

Allowing $t \to \infty$ and substituting (A.8) into (A.21), one gets

$$0 \leq \liminf_{t\to\infty} \frac{1}{t} \int_0^t \mathbb{E}(g(x(\tau), u(\tau), v(\tau)))\mathrm{d}\tau, \quad \text{a.s.}$$

On the other hand, we note that

$$g(x, u, v) \leq Z < +\infty \quad \forall (x, u, v) \in \mathbb{R} \times \mathbb{R}^2_+,$$

where $Z = \sup_{(x,u,v)\in\mathbb{R}\times\mathbb{R}^2_+} \{-\frac{\rho_6 m(\mathcal{R}-1)}{2} - \rho_3\rho_6(k-u)^2 + \frac{a^2bk^2\rho_2\rho_6}{4r\rho_4}v^2 + \theta(\bar{x}-x)(e^x - 1) + \frac{\sigma^2}{2}e^x - \frac{r}{2k}u^4 - \frac{m}{2b^3}v^3 + \rho_5\}$. Then we have

$$\begin{aligned}
&\liminf_{t\to\infty} \frac{1}{t} \int_0^t \mathbb{E}(g(x(\tau), u(\tau), v(\tau)))\mathrm{d}\tau \\
&\quad \leq Z \liminf_{t\to\infty} \frac{1}{t} \int_0^t \mathbf{1}_{\{(x(\tau),u(\tau),v(\tau))\in\mathbb{D}\}}\mathrm{d}\tau - \liminf_{t\to\infty} \frac{1}{t} \int_0^t \mathbf{1}_{\{(x(\tau),u(\tau),v(\tau))\in\mathbb{D}^c\}}\mathrm{d}\tau \\
&\quad \leq (Z+1) \liminf_{t\to\infty} \frac{1}{t} \int_0^t \mathbf{1}_{\{(x(\tau),u(\tau),v(\tau))\in\mathbb{D}\}}\mathrm{d}\tau - 1.
\end{aligned}$$

Therefore, we have

$$\liminf_{t\to\infty} \frac{1}{t} \int_0^t \mathbf{1}_{\{(x(\tau),u(\tau),v(\tau))\in\mathbb{D}\}}\mathrm{d}\tau \geq \frac{1}{Z+1} > 0, \quad \text{a.s.} \tag{A.22}$$

Following an analysis comparable to the existence and ergodicity of the solution found in [28], it is obtained that

$$\liminf_{t\to\infty} \frac{1}{t} \int_0^t \mathbb{P}(\tau, (x(\tau), u(\tau), v(\tau)), \mathbb{D})\mathrm{d}\tau \geq \frac{1}{Z+1} > 0, \quad \text{a.s.}, \tag{A.23}$$

where $\mathbb{P}(t, (x(t), u(t), v(t)), \mathbb{D})$ is the transition probability of $(x(t), u(t), v(t))$ belongs to the set $\mathbb{D}$. This implies that model (2.1) has at least one stationary distribution. This completes the proof. ∎

**A.3. Proof of Theorem 3.4.** The proof of Theorem 3.4 follows these steps:

*Step* 1. The kernel function of $(x(t), u(t), v(t))$ is shown to be absolutely continuous.

*Step* 2. Utilizing support theorems, it is established that the kernel function is positive on $\mathbb{S}$.

*Step* 3. It is demonstrated that the Markov semigroup exhibits asymptotic stability or sweeping behavior with respect to compact sets.

*Step* 4. The existence of a Khasminskii function is confirmed, which allows us to rule out the possibility of sweeping.

*Step* 1. Using Hörmander's condition [17, p. 228], we show that the transition function of the process $(x(t), u(t), v(t))$ is absolutely continuous.

LEMMA A.2. *For all* $(x_0, u_0, v_0)^\top \in \mathbb{R} \times \mathbb{S}$ *and* $t > 0$*, the transition probability function* $P(t, x_0, u_0, v_0, A)$ *possesses a continuous density* $h(t, x, u, v; x_0, u_0, v_0)$ *with respect to the Lebesgue measure.*

*Proof.* For a vector $\mathbf{y}$, let $\vec{\mathbf{a}}(\mathbf{y})$ and $\vec{\mathbf{b}}(\mathbf{y})$ be vector fields on $\mathbb{X}$ and the Lie bracket $[\vec{\mathbf{a}}, \vec{\mathbf{b}}]$ be a vector field given by

$$[\vec{\mathbf{a}}, \vec{\mathbf{b}}]_j(\mathbf{y}) = \sum_{i=1}^{3} \left( \mathbf{a}_i \frac{\partial \mathbf{b}_j}{\partial y_i}(\mathbf{y}) - \mathbf{b}_i \frac{\partial \mathbf{a}_j}{\partial y_i}(\mathbf{y}) \right), \quad j = 1, 2, 3.$$

Denote

$$\vec{\mathbf{a}}(x, u, v) = \begin{pmatrix} f_1(x) \\ f_2(x, u, v) \\ f_3(x, u, v) \end{pmatrix}, \quad \vec{\mathbf{b}}(x, u, v) = \begin{pmatrix} \sigma \\ 0 \\ 0 \end{pmatrix},$$

where $(x, u, v) \in \mathbb{X}$ and

$$f_1(x) = \theta(\bar{x} - x),\ f_2(x, u, v) = ru\left(1 - \frac{u}{k}\right) - ae^{cx}uv, f_2(x, u, v) = abe^{cx}uv - mv.$$

Letting $\vec{\zeta_1} \triangleq [\vec{\mathbf{a}}, \vec{\mathbf{b}}]$ and $\vec{\zeta_2} \triangleq [\vec{\mathbf{a}}, \vec{\mathbf{c}_1}]$, we have

$$\vec{\zeta_1} = \begin{pmatrix} \theta\sigma \\ \sigma ace^{cx}uv \\ -\sigma abce^{cx}uv \end{pmatrix}, \vec{\zeta_2} = \begin{pmatrix} \theta^2\sigma \\ \sigma ace^{cx}uv\left[\theta(1 + c\bar{x} - cx) + \frac{r}{k}u - m\right] \\ \sigma abce^{cx}uv\left[r - \theta(1 + c\bar{x} - cx) + \frac{r}{k}u\right] \end{pmatrix}.$$

Hence, we have

$$\left|\vec{b}, \vec{\zeta_1}, \vec{\zeta_2}\right| = \sigma^3 a^2 bc^2 e^{2cx} u^2 v^2 \left(\frac{2r}{k}u - r - m\right) < 0,$$

where the above inequality holds because $u < k$ and $r < m$. Therefore, for every $(x, u, v)^\top \in \mathbb{S}$, the vectors $\vec{\mathbf{b}}$, $\vec{\zeta_1}$, and $\vec{\zeta_2}$ span the space $\mathbb{S}$. In view of Hörmander's theorem [17, p. 228], the transition probability function $P(t, x_0, u_0, v_0, A)$ has a continuous density $h(t, x, u, v; x_0, u_0, v_0)$ and $h \in C^\infty((0, \infty) \times \mathbb{S})$. This completes the proof. ∎

*Step* 2. Using support theorems in [2], we prove that the density of the transition function is positive on $\mathbb{S}$.

LEMMA A.3. *For all* $(x_0, u_0, v_0)^\top \in \mathbb{S}$ *and* $(x_1, u_1, v_1)^\top \in \mathbb{S}$, *there exists* $\tau > 0$ *such that* $h(\tau, x_1, u_1, v_1; x_0, u_0, v_0) > 0$.

*Proof.* Fixing a point $(x_0, u_0, v_0) \in \mathbb{S}$ and a function $\phi \in L^2([0, \tau]; \mathbb{R})$, we consider the following integral equations:

$$\begin{cases} x_\phi(t) = x_0 + \displaystyle\int_0^t (f_1(x_\phi(s)) + \sigma\phi)\,\mathrm{d}s, \\ u_\phi(t) = u_0 + \displaystyle\int_0^t f_2(x_\phi(s), u_\phi(s), v_\phi(s))\mathrm{d}s, \\ v_\phi(t) = v_0 + \displaystyle\int_0^t f_3(x_\phi(s), u_\phi(s), v_\phi(s))\mathrm{d}s. \end{cases} \tag{A.24}$$

Let $D_{x_0,u_0,v_0;\phi}$ be the Frechét derivative of $\eta(\tau) \mapsto \begin{pmatrix} x_{\phi+\eta}(\tau) \\ u_{\phi+\eta}(\tau) \\ v_{\phi+\eta}(\tau) \end{pmatrix}$ from $L^2([0, \tau]; \mathbb{R})$ to $\mathbb{S}$. Denote

$$\Upsilon(t) = \begin{pmatrix} -\theta & 0 & 0 \\ -ace^{cx(t)}u(t)v(t) & r - \frac{2r}{k}u(t) - ae^{cx(t)}v(t) & -ae^{cx(t)}u(t) \\ abce^{cx(t)}u(t)v(t) & abe^{cx(t)}v(t) & abe^{cx(t)}u(t) - m \end{pmatrix}.$$

For $0 \le t_0 \le t \le \tau$, Let $Q(t,t_0)$ be a matrix function such that $Q(t_0,t_0) = \mathbf{I}_d$ and $\frac{\partial Q(t,t_0)}{\partial t} = \Upsilon(t)Q(t,t_0)$. Then we have $D_{x_0,u_0,v_0;\phi}\eta = \int_0^\tau Q(\tau,s)g(s)\eta(s)\mathrm{d}s$. To prove the rank of $D_{x_0,u_0,v_0;\phi}$ is 3, we let $\tau_1 \in (0,\tau)$ and $\eta(t) = \mathbf{1}_{[\tau-\tau_1,\tau]}(t)$, $t \in [0,\tau]$. Making the use of Taylor expansion, we obtain

$$Q(\tau,\varepsilon) = \mathbf{I}_d + \Upsilon(\tau)(\varepsilon-\tau) + \frac{1}{2}\Upsilon^2(\tau)(\varepsilon-\tau)^2 + o((\varepsilon-\tau)^2).$$

Hence, $D_{x_0,u_0,v_0;\phi}\eta = \tau_1\boldsymbol{\sigma} - \frac{\tau_1^2}{2}\Upsilon(\tau)\boldsymbol{\sigma} + \frac{\tau_1^3}{6}\Upsilon^2(\tau)\boldsymbol{\sigma} + o(\tau_1^3)$, with $\boldsymbol{\sigma} = (-\sigma,0,0)^\top$. Then direct calculations lead to

$$\Upsilon(\tau)\boldsymbol{\sigma} = \begin{pmatrix} -\theta\sigma \\ -\sigma ace^{cx}uv \\ \sigma abce^{cx}uv \end{pmatrix},\ \Upsilon^2(\tau)\boldsymbol{\sigma} = \begin{pmatrix} \theta^2\sigma \\ \sigma ace^{cx}uv\left(\frac{2r}{k} + \theta + ae^{cx}v - abe^{cx}u\right) \\ -\sigma abce^{cx}uv\left[\theta + ae^{cx}v + m - abe^{cx}u\right] \end{pmatrix}.$$

Hence, $|\boldsymbol{\sigma}, \Upsilon(\tau)\boldsymbol{\sigma}, \Upsilon^2(\tau)\boldsymbol{\sigma}| = \sigma^3a^2bc^2e^{2cx}u^2v^2(r+m-\frac{2r}{k}u) > 0$, where the inequality holds because $u < k$ and $r < m$. This implies that $h(\tau,x,u,v;x_0,u_0,v_0) > 0$ for $(x,u,v) = (x_\phi(\tau),u_\phi(\tau),v_\phi(\tau))$ due to the vectors $\boldsymbol{\sigma}$, $\Upsilon(\tau)\boldsymbol{\sigma}$, $\Upsilon^2(\tau)\boldsymbol{\sigma}$ being linearly independent and the rank of $D_{x_0,u_0,v_0;\phi}$ being 3.

Next, we show that for any two points $(x_0,u_0,v_0)$ and $(x_1,u_1,v_1)$ in $\mathbb{S}$, there exist a control function $\phi$ and $\tau > 0$ such that $x_\phi(0) = x_0$, $u_\phi(0) = u_0$, $v_\phi(0) = v_0$, $x_\phi(\tau) = x_1$, $u_\phi(\tau) = u_1$, and $v_\phi(\tau) = v_1$.

Letting $w_\phi = u_\phi + \frac{v_\phi}{b}$, from (A.24), one can obtain

$$\dot{w}_\phi = ru_\phi\left(1 - \frac{u_\phi}{k}\right) - bm(w_\phi - u_\phi) = f_4(u_\phi) - bmw_\phi, \tag{A.25}$$

where $f_4(u_\phi) = (r+bm)u_\phi - \frac{r}{k}u_\phi^2$, which is monotonically increasing for $u_\phi \in (0,k)$. From (A.25), we have $u_\phi = f_4^{-1}(\dot{w}_\phi + bmw_\phi)$. Furthermore, one gets

$$v_\phi = b(w_\phi - u_\phi) = b(w_\phi - f_4^{-1}(\dot{w}_\phi + bmw_\phi)).$$

In order to ensure $e^{x_\phi} > 0$, according to $f_2(x,u,v)$, it is necessary that

$$e^{x_\phi} = \frac{1}{au_\phi v_\phi}\left[ru_\phi\left(1 - \frac{u_\phi}{k}\right) - \dot{u}_\phi\right] > 0.$$

By combining $w_\phi - f_4^{-1}(\dot{w}_\phi + bmw_\phi) > 0$, it follows that $\dot{w}_\phi + bmw_\phi < f_4(w_\phi) = (r+bm)w_\phi - \frac{r}{k}w_\phi^2$. Thus, the control function $\phi$ only needs to satisfy the following conditions:

$$\begin{cases} -bmw_\phi < \dot{w}_\phi < rw_\phi\left(1 - \frac{w_\phi}{k}\right), \\ u_\phi = f_3^{-1}(\dot{w}_\phi + bmw_\phi), \\ \dot{u}_\phi < ru_\phi\left(1 - \frac{u_\phi}{k}\right). \end{cases} \tag{A.26}$$

First we construct the control function $x_\phi$:

$$x_\phi(t) = \begin{cases} x(0) + \dfrac{\tilde{x} - x(0)}{\tau_1}t, & t \in [0,\tau_1), \\ \tilde{x}, & t \in [\tau_1,\tau_2), \end{cases}$$

where $\tilde{x} > \frac{m}{abk}$ is a constant, $0 < \tau_1 < \tau_2$, and $\tau_2$ is a constant such that $|\dot{u}_\phi(\tau_2)| < \epsilon$, $|\dot{v}_\phi(\tau_2)| < \epsilon$ and $|u_\phi(\tau_2) - \tilde{u}| < \epsilon$, $|v_\phi(\tau_2) - \tilde{v}| < \epsilon$ $\forall \epsilon > 0$ with

$$\tilde{u} = \frac{m}{abe^{c\tilde{x}}}, \quad \tilde{v} = \frac{(k-\tilde{u})r}{ake^{c\tilde{x}}}.$$

Similarly, define

$$x_\phi(t) = \begin{cases} x_1 + \dfrac{\tilde{x} - x_1}{\tau_4}(\tau - t), & t \in (\tau - \tau_4, \tau], \\ \tilde{x}, & t \in (\tau_3, \tau - \tau_4], \end{cases}$$

such that $|\dot{u}_\phi(\tau_3)| < \epsilon$, $|\dot{v}_\phi(\tau_3)| < \epsilon$ and $|u_\phi(\tau_3) - \tilde{u}| < \epsilon$, $|v_\phi(\tau_3) - \tilde{v}| < \epsilon$ $\forall \epsilon > 0$. Define

$$x_\phi(t) \equiv \tilde{x}, \quad u_\phi(t) \equiv \tilde{u}, \quad v_\phi(t) \equiv \tilde{v} \quad \text{for } t \in (\tau_2, \tau_3).$$

Hence, it follows that there exists a continuous control function $\phi$ that satisfies (A.26). Furthermore, the continuous control function $\phi$ satisfies that $x_\phi(0) = x_0$, $u_\phi(0) = u_0$, $v_\phi(0) = v_0$, $x_\phi(T) = x_1$, $u_\phi(T) = u_1$, and $v_\phi(T) = v_1$ for $T > 0$. This completes the proof. ∎

*Step* 3. We show that the Markov semigroup is asymptotically stable or is sweeping concerning compact sets.

LEMMA A.4. *The semigroup $\{P(t)\}_{t\geq 0}$, given as a Markov semigroup in* [41]*, is either asymptotically stable or sweeping with respect to compact sets.*

*Proof.* By virtue of Lemma A.2, we can get that the semigroup $\{P(t)\}_{t\geq 0}$ is integral with a continuous density $h(t, u, v, w)$ for $t > 0$. By Lemma A.3, for every density $h \in \mathbb{S}$, we obtain

$$\int_0^\infty P(t)h\mathrm{d}t > 0, \quad \text{a.e. on } \mathbb{S},$$

due to $h(t, u, v, w) > 0$ and $P(t)h = \int_{\mathbb{S}} h(t, \boldsymbol{z})h(\boldsymbol{z})\beta(\mathrm{d}\boldsymbol{z})$, where $\boldsymbol{z} = (x, u, v)^\top$. Thus, in view of Lemma 3 in [41], we can derive that the Markov semigroup $\{P(t)\}_{t\geq 0}$ is asymptotically stable or sweeping with respect to compact sets. This completes the proof. ∎

*Step* 4. For the sake of excluding sweeping, we prove the existence of the Khasminskiĭ function.

LEMMA A.5. *If $\mathcal{R} > 1$ and $m > r$, then the semigroup $\{P(t)\}_{t\geq 0}$ is asymptotically stable.*

*Proof.* According to the previous lemma, the semigroup $\{P(t)\}_{t\geq 0}$ satisfies the Foguel alternative. Using the function $W_5$ and the closed set $\mathbb{D}$ defined in Appendix A.2, we can exclude the possibility of sweeping. According to Lemma 3 in [41], $\{P(t)\}_{t\geq 0}$ is asymptotically stable. This completes the proof. ∎

### A.4. Proof of Theorem 3.5.

*Proof.* First we can obtain that a quasi-positive equilibrium $E^* = (\bar{x}, u^*, v^*)$ exists when $abke^{c\bar{x}} > m$. Then let $u_1 = u - u^*$ and $v_1 = v - v^*$. Applying Itô's integral, the corresponding linearized system of model (2.1) around $E^*$ is as follows:

$$\mathrm{d}Y(t) = AY(t)\mathrm{d}t + \Theta \mathrm{d}B(t), \tag{A.27}$$

where $Y = (x_1, u_1, v_1)^\top$, $\Theta = \mathrm{diag}(\sigma, 0, 0)$, and

$$A = \begin{pmatrix} -\theta & 0 & 0 \\ -ace^{c\bar{x}}u^*v^* & -\frac{ru^*}{k} & -ae^{c\bar{x}}u^* \\ abce^{c\bar{x}}u^*v^* & abe^{c\bar{x}}v^* & 0 \end{pmatrix}.$$

By applying the results from Øksendal [33] and Mao [27], it follows that the system (A.27) has a unique explicit solution:

$$Y(t) = Y(0)e^{At} + \int_0^t e^{A(t-s)}\Theta \mathrm{d}B(t). \tag{A.28}$$

Note that the martingale $\int_0^t e^{A(t-s)}\Theta \mathrm{d}B(t)$ follows a Gaussian distribution $\mathbb{N}((0,0,0)^\top, \tilde{\Sigma}(t))$, where $\tilde{\Sigma}(t) = \int_0^t e^{A^\top(t-s)}\Theta^2 e^{A(t-s)}\mathrm{d}s$. In addition, the characteristic polynomial of $A$ is $\psi_A(\lambda) = (\lambda+\theta)(\lambda^2+\frac{ru^*}{k}\lambda+a^2be^{2c\bar{x}}u^*v^*)$. According to the Routh–Hurwitz criterion, all roots of $\psi_A(\lambda)$ have negative real parts. Thus, we have

$$\lim_{t\to\infty} e^{At} = 0, \quad \Sigma = \lim_{t\to\infty}\tilde{\Sigma}(t) = \int_0^\infty e^{A^\top t}\Theta^2 e^{At}\mathrm{d}t. \tag{A.29}$$

It can be calculated that

$$\frac{\mathrm{d}}{\mathrm{d}t}\left(\int_0^\infty e^{A^\top t}\Theta^2 e^{At}\mathrm{d}t\right) = A\Sigma + \Sigma A^\top, \quad \int_0^\infty \frac{\mathrm{d}}{\mathrm{d}t}\left(e^{A^\top t}\Theta^2 e^{At}\mathrm{d}t\right) = \Theta^2.$$

Based on the continuity of the matrix function, we obtain that

$$\Theta^2 + A\Sigma + \Sigma A^\top = 0. \tag{A.30}$$

Then we have

$$A_1 = T_1 A T_1^{-1} = \begin{pmatrix} -\theta & 0 & 0 \\ -ace^{c\bar{x}}u^*v^* & -\frac{r}{k} + ae^{c\bar{x}}v^* & -ae^{c\bar{x}}u^* \\ 0 & a_4 & -abe^{c\bar{x}}u^* \end{pmatrix}.$$

Furthermore, one gets

$$A_2 = T_2 A_1 T_2^{-1} = \begin{pmatrix} -a_1 & -a_2 & -a_3 \\ 1 & 0 & 0 \\ 0 & 1 & 0 \end{pmatrix}.$$

Thus, $(T_2T_1)\Theta^2(T_2T_1)^\top + A_2[(T_2T_1)\Sigma(T_2T_1)^\top] + [(T_2T_1)\Sigma(T_2T_1)^\top]A_2^\top = 0$. Since $a_1a_2 - a_3 = \frac{(a_2+\theta^2)r}{k} > 0$, we obtain that $(T_2T_1)\Sigma(T_2T_1)^\top = (abcm\sigma e^{c\bar{x}}u^*v^*)^2\Omega$ is a positive definite symmetric matrix from Theorem 3.1 in [58]. Therefore, we obtain that $\Sigma = (abcm\sigma e^{c\bar{x}}u^*v^*)^2(T_2T_1)^{-1}\Omega[(T_2T_1)^{-1}]^\top$ is positive definite. This completes the proof. ∎

## REFERENCES


[1] E. Allen, *Environmental variability and mean-reverting processes*, Discrete Contin. Dyn. Syst. Ser. B, 21 (2016), pp. 2073–2089, https://doi.org/10.3934/dcdsb.2016037.

[2] G. B. Arous and R. Léandre, *Décroissance exponentielle du noyau de la chaleur sur la diagonale* (II), Probab. Theory Related Fields, 90 (1991), pp. 377–402, https://doi.org/10.1007/BF01193751.

[3] A. Attanasi, A. Cavagna, L. Del Castello, I. Giardina, S. Melillo, L. Parisi, O. Pohl, B. Rossaro, E. Shen, E. Silvestri, and M. Viale, *Collective behaviour without collective order in wild swarms of midges*, Plos Comput. Biol., 10 (2014), e1003697, https://doi.org/10.1371/journal.pcbi.1003697.

[4] R. G. Barry, *Mountain Weather and Climate*, Routledge, 2013.

[5] G. Berthelot, S. Saïd, and V. Bansaye, *A random walk model that accounts for space occupation and movements of a large herbivore*, Sci. Rep., 11 (2021), 14061, https://doi.org/10.1038/s41598-021-93387-2.

[6] W. Bialek, A. Cavagna, I. Giardina, T. Mora, E. Silvestri, M. Viale, and A. M. Walczak, *Statistical mechanics for natural flocks of birds*, Proc. Natl. Acad. Sci. USA, 109 (2012), pp. 4786–4791, https://doi.org/10.1073/pnas.1118633109.

[7] P. Blackwell, *Random diffusion models for animal movement*, Ecol. Model., 100 (1997), pp. 87–102, https://doi.org/10.1016/S0304-3800(97)00153-1.

[8] G. A. Breed, E. A. Golson, and M. T. Tinker, *Predicting animal home-range structure and transitions using a multistate Ornstein-Uhlenbeck biased random walk*, Ecology, 98 (2017), pp. 32–47, https://doi.org/10.1002/ecy.1615.

[9] D. S. Callaway and A. Hastings, *Consumer movement through differentially subsidized habitats creates a spatial food web with unexpected results*, Ecol. Lett., 5 (2002), pp. 329–332, https://doi.org/10.1046/j.1461-0248.2002.00330.x.

[10] S. Camazine, P. K. Visscher, J. Finley, and R. S. Vetter, *House-hunting by honey bee swarms: Collective decisions and individual behaviors*, Insect. Soc., 46 (1999), pp. 348–360, https://doi.org/10.1007/s000400050156.

[11] A. I. Dell, S. Pawar, and V. M. Savage, *Systematic variation in the temperature dependence of physiological and ecological traits*, Proc. Natl. Acad. Sci. USA, 108 (2011), pp. 10591–10596, https://doi.org/10.1073/pnas.1015178108.

[12] J. E. Dunn and P. S. Gipson, *Analysis of radio telemetry data in studies of home range*, Biometrics, 33 (1977), 85, https://doi.org/10.2307/2529305.

[13] L. Dyson, C. A. Yates, C. Buhl, and A. J. McKane, *Onset of collective motion in locusts is captured by a minimal model*, Phys. Rev. E (3), 92 (2015), 052708, https://doi.org/10.1103/PhysRevE.92.052708.

[14] J. M. Eisaguirre, T. L. Booms, C. P. Barger, S. D. Goddard, and G. A. Breed, *Multistate Ornstein–Uhlenbeck approach for practical estimation of movement and resource selection around central places*, Methods Ecol. Evol., 12 (2021), pp. 507–519, https://doi.org/10.1111/2041-210X.13538.

[15] J. M. Eisaguirre, T. L. Booms, C. P. Barger, S. B. Lewis, and G. A. Breed, *Demographic partitioning of dynamic energy subsidies revealed with an Ornstein–Uhlenbeck space use model*, Ecol. Appl., 32 (2022), e2542, https://doi.org/10.1002/eap.2542.

[16] P. Fauchald, *Spatial interaction between seabirds and prey: Review and synthesis*, Marine Ecol. Progress Series, 391 (2009), pp. 139–151, https://doi.org/10.3354/meps07818.

[17] P. Garbaczewski and R. Olkiewicz, *Dynamics of Dissipation*, Lecture Notes in Phys. 597, Springer, Berlin, New York, 2002.

[18] J. F. Gillooly, J. H. Brown, G. B. West, V. M. Savage, and E. L. Charnov, *Effects of size and temperature on metabolic rate*, Science, 293 (2001), pp. 2248–2251, https://doi.org/10.1126/science.1061967.

[19] A. Hastings, *Global stability of two species systems*, J. Math. Biol., 5 (1977), pp. 399–403, https://doi.org/10.1007/BF00276109.

[20] S. Herrmann and N. Massin, *Exit problem for Ornstein-Uhlenbeck processes: A random walk approach*, Discrete Contin. Dyn. Syst. Ser. B, 25 (2020), pp. 3199–3215, https://doi.org/10.3934/dcdsb.2020058.

[21] D. J. Higham, *An algorithmic introduction to numerical simulation of stochastic differential equations*, SIAM Rev., 43 (2001), pp. 525–546, https://doi.org/10.1137/S0036144500378302.

[22] H. Jenny, *Factors of Soil Formation: A System of Quantitative Pedology*, Courier Corporation, 1994.

[23] J. Jhawar, R. G. Morris, U. R. Amith-Kumar, M. Danny Raj, T. Rogers, H. Rajendran, and V. Guttal, *Noise-induced schooling of fish*, Nat. Phys., 16 (2020), pp. 488–493, https://doi.org/10.1038/s41567-020-0787-y.

[24] J. T. Kirk, *Light and Photosynthesis in Aquatic Ecosystems*, Cambridge University Press, 1994.

[25] K. J. Laidler, *The development of the Arrhenius equation*, J. Chem. Educ., 61 (1984), 494, https://doi.org/10.1021/ed061p494.

[26] S. A. Levin and L. A. Segel, *Hypothesis for origin of planktonic patchiness*, Nature, 259 (1976), 659, https://doi.org/10.1038/259659a0.

[27] X. Mao, *Stochastic Differential Equations and Applications*, 2nd ed., Horwood, Chichester, 2008.

[28] S. P. Meyn and R. L. Tweedie, *Stability of Markovian processes* III*: Foster–Lyapunov criteria for continuous-time processes*, Adv. Appl. Probab., 25 (1993), pp. 518–548, https://doi.org/10.2307/1427522.

[29] A. T. Moles, D. I. Warton, L. Warman, N. G. Swenson, S. W. Laffan, A. E. Zanne, A. Pitman, F. A. Hemmings, and M. R. Leishman, *Global patterns in plant height*, J. Ecol., 97 (2009), pp. 923–932, https://doi.org/10.1111/j.1365-2745.2009.01526.x.

[30] T. Mueller and W. F. Fagan, *Search and navigation in dynamic environments–from individual behaviors to population distributions*, Oikos, 117 (2008), pp. 654–664, https://doi.org/10.1111/j.0030-1299.2008.16291.x.

[31] R. Nathan, W. M. Getz, E. Revilla, M. Holyoak, R. Kadmon, D. Saltz, and P. E. Smouse, *A movement ecology paradigm for unifying organismal movement research*, Proc. Natl. Acad. Sci. USA, 105 (2008), pp. 19052–19059, https://doi.org/10.1073/pnas.0800375105.

[32] M. I. O'Connor, B. Gilbert, and C. J. Brown, *Theoretical predictions for how temperature affects the dynamics of interacting herbivores and plants*, Amer. Natural., 178 (2011), pp. 626–638, https://doi.org/10.1086/662171.

[33] B. Øksendal, *Stochastic Differential Equations*, Universitext, Springer, Berlin, Heidelberg, 2003, https://doi.org/10.1007/978-3-642-14394-6.

[34] A. Okubo, *Dynamical aspects of animal grouping: Swarms, schools, flocks, and herds*, Adv. Biophys., 22 (1986), pp. 1–94, https://doi.org/10.1016/0065-227X(86)90003-1.

[35] D. J. G. Pearce, A. M. Miller, G. Rowlands, and M. S. Turner, *Role of projection in the control of bird flocks*, Proc. Natl. Acad. Sci. USA, 111 (2014), pp. 10422–10426, https://doi.org/10.1073/pnas.1402202111.

[36] S. Peng and X. Zhu, *Necessary and sufficient condition for comparison theorem of 1-dimensional stochastic differential equations*, Stochastic Process. Appl., 116 (2006), pp. 370–380, https://doi.org/10.1016/j.spa.2005.08.004.

[37] O. Petit and R. Bon, *Decision-making processes: The case of collective movements*, Behav. Process., 84 (2010), pp. 635–647, https://doi.org/10.1016/j.beproc.2010.04.009.

[38] H. Poorter, K. J. Niklas, P. B. Reich, J. Oleksyn, P. Poot, and L. Mommer, *Biomass allocation to leaves, stems and roots: Meta-analyses of interspecific variation and environmental control*, New Phytologist, 193 (2012), pp. 30–50.

[39] H. K. Preisler, A. A. Ager, B. K. Johnson, and J. G. Kie, *Modeling animal movements using stochastic differential equations*, Environmetrics, 15 (2004), pp. 643–657, https://doi.org/10.1002/env.636.

[40] A. M. Reynolds, *Intrinsic stochasticity and the emergence of collective behaviours in insect swarms*, European Phys. J. E, 44 (2021), 22, https://doi.org/10.1140/epje/s10189-021-00040-x.

[41] R. Rudnicki and K. Pichór, *Influence of stochastic perturbation on prey–predator systems*, Math. Biosci., 206 (2007), pp. 108–119, https://doi.org/10.1016/j.mbs.2006.03.006.

[42] M. Scheffer, S. Carpenter, J. A. Foley, C. Folke, and B. Walker, *Catastrophic shifts in ecosystems*, Nature, 413 (2001), pp. 591–596, https://doi.org/10.1038/35098000.

[43] P. M. Schulte, *The effects of temperature on aerobic metabolism: Towards a mechanistic understanding of the responses of ectotherms to a changing environment*, J. Exp. Biol., 218 (2015), pp. 1856–1866, https://doi.org/10.1242/jeb.118851.

[44] Y. Shemesh, Y. Sztainberg, O. Forkosh, T. Shlapobersky, A. Chen, and E. Schneidman, *High-order social interactions in groups of mice*, eLife, 2 (2013), e00759, https://doi.org/10.7554/eLife.00759.

[45] Q. Shi, Y. Song, and H. Wang, *Local perception and learning mechanisms in resource-consumer dynamics*, SIAM J. Appl. Math., 84 (2024), pp. 988–1010, https://doi.org/10.1137/23M1598593.

[46] Z. Shi and D. Jiang, *A viral co-infection model with general infection rate in deterministic and stochastic environments*, Commun. Nonlinear Sci., 126 (2023), 107436, https://doi.org/10.1016/j.cnsns.2023.107436.

[47] I. Silva, C. H. Fleming, M. J. Noonan, J. Alston, C. Folta, W. F. Fagan, and J. M. Calabrese, *Autocorrelation-informed home range estimation: A review and practical guide*, Methods Ecol. Evol., 13 (2022), pp. 534–544, https://doi.org/10.1111/2041-210X.13786.

[48] J. S. Singh, *Forests of Himalaya: Structure, Functioning and Impact of Man*, CGyanodaya Prakashan, 1992.

[49] N. Sk, P. K. Tiwari, Y. Kang, and S. Pal, *A nonautonomous model for the interactive effects of fear, refuge and additional food in a prey–predator system*, J. Biol. Syst., 29 (2021), pp. 107–145, https://doi.org/10.1142/S0218339021500054.

[50] P. E. Smouse, S. Focardi, P. R. Moorcroft, J. G. Kie, J. D. Forester, and J. M. Morales, *Stochastic modelling of animal movement*, Philos. Trans. Roy. Soc. B: Biol. Sci., 365 (2010), pp. 2201–2211, https://doi.org/10.1098/rstb.2010.0078.

[51] Y. Song, H. Wang, and J. Wang, *Cognitive consumer-resource spatiotemporal dynamics with nonlocal perception*, J. Nonlinear Sci., 34 (2024), 19, https://doi.org/10.1007/s00332-023-09996-w.

[52] T. Székely and K. Burrage, *Stochastic simulation in systems biology*, Comput. Struct. Biotechnol. J., 12 (2014), pp. 14–25, https://doi.org/10.1016/j.csbj.2014.10.003.

[53] D. A. Vasseur and K. S. McCann, *A mechanistic approach for modeling temperature-dependent consumer-resource dynamics*, Amer. Natural., 166 (2005), pp. 184–198, https://doi.org/10.1086/431285.

[54] H. Wang and Y. Salmaniw, *Open problems in PDE models for knowledge-based animal movement via nonlocal perception and cognitive mapping*, J. Math. Biol., 86 (2023), 71, https://doi.org/10.1007/s00285-023-01905-9.

[55] M. Y. Li, X. Lin, and H. Wang, *Global Hopf branches and multiple limit cycles in a delayed Lotka-Volterra predator-prey model*, Discrete Contin. Dyn. Syst. Ser. B, 19 (2014), pp. 747–760, https://doi.org/10.3934/dcdsb.2014.19.747.

[56] C. A. Yates, R. Erban, C. Escudero, I. D. Couzin, C. Buhl, I. G. Kevrekidis, P. K. Maini, and D. J. T. Sumpter, *Inherent noise can facilitate coherence in collective swarm motion*, Proc. Natl. Acad. Sci. USA, 106 (2009), pp. 5464–5469, https://doi.org/10.1073/pnas.0811195106.

[57] B. Zhou, D. Jiang, B. Han, and T. Hayat, *Threshold dynamics and density function of a stochastic epidemic model with media coverage and mean-reverting Ornstein–Uhlenbeck process*, Math. Comput. Simul., 196 (2022), pp. 15–44, https://doi.org/10.1016/j.matcom.2022.01.014.

[58] B. Zhou, H. Wang, T. Wang, and D. Jiang, *Stochastic generalized Kolmogorov systems with small diffusion:* I. *Explicit approximations for invariant probability density function*, J. Differential Equations, 382 (2024), pp. 141–210, https://doi.org/10.1016/j.jde.2023.10.057.